



HAL
open science

Deciphering the properties of hemp seed oil bodies for food applications: Lipid composition, microstructure, surface properties and physical stability

Christelle Lopez, Bruno Novales, Hanitra Rabesona, Magalie Weber, Thierry Chardot, Marc Anton

► To cite this version:

Christelle Lopez, Bruno Novales, Hanitra Rabesona, Magalie Weber, Thierry Chardot, et al.. Deciphering the properties of hemp seed oil bodies for food applications: Lipid composition, microstructure, surface properties and physical stability. *Food Research International*, 2021, 150, pp.110759. 10.1016/j.foodres.2021.110759 . hal-03465007

HAL Id: hal-03465007

<https://hal.inrae.fr/hal-03465007v1>

Submitted on 5 Jan 2024

HAL is a multi-disciplinary open access archive for the deposit and dissemination of scientific research documents, whether they are published or not. The documents may come from teaching and research institutions in France or abroad, or from public or private research centers.

L'archive ouverte pluridisciplinaire **HAL**, est destinée au dépôt et à la diffusion de documents scientifiques de niveau recherche, publiés ou non, émanant des établissements d'enseignement et de recherche français ou étrangers, des laboratoires publics ou privés.



Distributed under a Creative Commons Attribution - NonCommercial 4.0 International License

1

2 **Deciphering the properties of hemp seed oil bodies for food applications:**
3 **lipid composition, microstructure, surface properties and physical stability**

4

5 Christelle Lopez ^{1*}, Bruno Novales ^{1,2}, Hanitra Rabesona¹, Magalie Weber ¹, Thierry Chardot ³, Marc
6 Anton ¹

7

8 ¹INRAE, UR BIA, F-44316, Nantes, France

9 ²INRAE, BIBS facility, F-44316, Nantes, France

10 ³INRAE, AgroParisTech, Université Paris-Saclay, Institut Jean-Pierre Bourgin, F-78000 Versailles,
11 France

12

13 *Corresponding author: Christelle Lopez

14 Christelle.lopez@inrae.fr

15

16

17 Abstract

18 Hemp seed oil bodies (HSOBs) are of growing interest in response to the demand of consumers for
19 healthy and natural plant-based food formulations. In this study, we used minimal processing
20 including aqueous extraction by grinding and centrifugation to obtain HSOBs. We determined the
21 lipid composition of HSOBs, their microstructure, and the impact of the homogenization pressure, pH
22 and minerals on their surface properties and the physical stability of the emulsions. HSOBs contain
23 high levels of well-balanced PUFA with LA/ALA=2.9, γ -tocopherol, lutein and phytosterols. The mean
24 diameter of HSOBs was $2.3 \pm 0.1 \mu\text{m}$ with an isoelectric point in the range of pH 4.4 to 4.6.
25 Homogenisation of hemp seed extracts induced a decrease in the size of HSOBs but did not eliminate
26 the sedimentation of the protein bodies composed of the globulin edestin. By changing the surface
27 properties of HSOBs, pH values below 6 and NaCl induced the aggregation of HSOBs, while CaCl_2
28 induced both aggregation and membrane-fusion mediated coalescence of HSOBs by involving
29 probably the anionic phospholipids together to membrane proteins. This study will contribute to
30 extend the range of novel food products and designed emulsions containing hemp seed proteins and
31 OBs.

32

33 **Keywords:** lipid droplet, oil body, interface, membrane, natural oil in water emulsion,
34 homogenization, plant based food source

35

36 1. Introduction

37 Consumers do expect more natural, minimally processed, of high sensorial quality, nutritionally
38 interesting, and healthy food products (Battacchi et al., 2020; Román et al., 2017). The ever-
39 increasing demand of consumers for plant-based diets, including foods containing plant-based
40 proteins of nutritional interest and lipids rich in polyunsaturated fatty acids (PUFA; mainly *n*-3 FA)
41 and other bioactive compounds, is in the spotlight and has made it essential to find and characterize
42 additional sources of plant nutrients. Oilseeds are among the most promising sustainable plant-based

43 food sources since they contain proteins and lipids in the form of natural oil bodies (OBs; also called
44 lipid droplets, oil droplets or oleosomes), both of which are essential for structuring food systems
45 such as emulsions and emulsion filled gels and for providing nutrients.

46 In this food transition context promoting sustainable diets, there has been a growing interest in the
47 last decade for hemp (*Cannabis Sativa L.*). Hemp cultivation has a low environmental impact and is
48 adapted to mild climate, whole hemp can be valorized and provides hemp seeds of nutritional
49 interest and health benefits (Farinon et al., 2020; Rupasinghe et al., 2020; Sorrentino, 2021). Hemp
50 seeds typically contain 25-35% lipids with over 80% amount of PUFA and a unique and perfectly
51 balanced essential fatty acid composition, i.e. ratio *n*-6 linoleic acid / *n*-3 α -linolenic acid around 3 as
52 recommended for human nutrition (Simopoulos, 2002). Hemp seeds also contain 20-25% proteins
53 (65-75% of globulin edestin, water-soluble albumins) of high biological value, easy to digest and rich
54 in essential amino acids, 20-30% carbohydrates (with mainly insoluble dietary fibre), as well as
55 vitamins and minerals (Farinon et al., 2020). Hemp seeds are praised for providing adequate
56 quantities of different nutrients to satisfy human dietary requirements (Rupasinghe et al., 2020).
57 Currently, hemp seeds are processed mainly by cold mechanical pressing or with the use of organic
58 solvents such as hexane to maximize the extraction yield of the valuable hemp oil and valorize the
59 hemp proteins by extraction from the cakes and transformation into powdered ingredients (hemp
60 protein concentrates or isolates) (Potin and Saurel, 2020).

61 Over the last two decades, the scientists and food manufacturers have increased their interest in the
62 natural properties of biological entities of plant origin such as the OBs, which can be recovered along
63 with proteins by aqueous extraction from seeds (Ntone et al., 2020). OBs are lipid-based nature-
64 assembled colloidal structures synthetised by plants to store the energy they need for germination
65 and growth. They are naturally designed to deliver nutrients, mainly the triacylglycerols (TAG), and
66 other biological components of nutritional and health interests (Acevedo-Fani et al., 2020). OBs could
67 therefore be further valorized in human diet, for example in complex food systems such as fermented
68 products, in response to the need of consumers to find green, biocompatible and natural

69 components in their diet. The use of natural OBs was suggested for dressings, sauces, dips, beverages
70 and desserts (Nikiforidis et al., 2014), and plant-based emulsion products such as mayonnaise
71 (Romero-Guzmán et al., 2020). However, the current lack of understanding of the microstructure and
72 surface properties of OBs in response to changes in pH and mineral environment, associated to the
73 physical stability of the emulsion poses a significant barrier to the development of OBs-based new
74 food products.

75 OBs are naturally emulsified delivery systems for a number of bioactive molecules including PUFA,
76 tocopherols, carotenoids and phytosterols. The structure of mature OBs consists of a central
77 hydrophobic core containing plant TAG (up to 94-98 wt%) and sterol esters. The TAG core is
78 stabilized by a complex interfacial layer consisting of 0.6 – 2 wt% phospholipids and 0.6 – 3 wt%
79 specialized integral membrane proteins such as the oleosins (15-26 kDa), the calcium-binding
80 caleosins (25-35 kDa) and steroleosins (40-60 kDa) (Nikiforidis et al., 2014; Tzen et al., 1993). As the
81 main membrane proteins, oleosins play a key role in the physical stabilization of the OBs against
82 coalescence by electrostatic repulsion and steric effects (Maurer et al., 2013). The interfacial
83 structure of OBs is further reinforced by electrostatic interactions between the positively charged
84 residues of the oleosins and the negatively charged groups of the phospholipids (White et al., 2008).
85 The naturally-occurring interface, mainly composed of membrane proteins and phospholipids,
86 protects the TAG core of OBs from oxidation, rendering the use of antioxidant agents unnecessary
87 (Kapchie et al., 2013).

88 Oil-in-water emulsions in foods can be exposed to different pH values and mineral stressful
89 conditions (e.g. presence of calcium) that could affect their physical stability through several
90 mechanisms including creaming, flocculation, and coalescence. The applications of natural OBs as
91 functional ingredients are closely related to their physical stability in foods. A fundamental
92 understanding of the physical stability of natural emulsions containing hemp seed OBs, under
93 variable conditions such as pH and ionic strength, would allow their incorporation into selected food
94 systems.

95 The objectives of this work were to characterize the lipid composition of natural OBs obtained by
96 minimal processing including aqueous extraction from hemp seeds, to examine their microstructure,
97 and to determine the impact of homogenisation, pH and minerals (various NaCl and CaCl₂
98 concentrations) on their surface properties and the physical stability of the emulsions.

99

100 **2. Materials and methods**

101 **2.1. Materials**

102 Whole hemp (*Cannabis sativa L.*) mature seeds from organic agriculture were produced by Nunti-
103 Sanya (Les chanvres de l'Atlantique, Saint Geours de Maremne, France), and purchased from Biocoop
104 (Landivisiau, France). The composition of the hemp seeds as provided by the seed producer was as
105 follows: proteins = 21 g/100 g ; carbohydrates = 7.4 g/100 g ; fibers = 30.6 g/100 g ; lipids = 31.2
106 g/100 g. The classes of fatty acids (FA) were as follows: saturated FA 3.3 g/100 g, monounsaturated
107 FA 5.6 g/100 g, polyunsaturated FA 22.3 g/100 g with linoleic acid 18:2n-6 (LA) 16.3 g/100 g and
108 alpha-linolenic acid 18:3n-3(ALA) 5.7 g/100 g and the LA/ALA ratio = 2.9.

109 Sodium chloride (NaCl) and calcium chloride (CaCl₂) were obtained in analytical grade from Sigma-
110 Aldrich (St Louis, MO, USA). D(+)-sucrose was purchased from VWR Chemicals (St Louis, USA).
111 Ultrapure (milliQ) water filtered with a Merck Millipore device (Darmstadt, Germany) was used to
112 perform the aqueous extractions, to recover oil bodies and protein bodies, and to dilute samples
113 where appropriate.

114

115 **2.2. Samples preparation**

116 **2.2.1. Oil body aqueous extraction**

117 Oil bodies were recovered from hemp seeds by applying aqueous extraction associated to a
118 mechanical treatment. Hemp seeds (batches of 100 g) were soaked in ultrapure water (1:3 w/v) for
119 20h at 20°C to allow their hydration. After soaking, the dispersion of seeds in water was ground for 3
120 min at a speed of 6000 rpm (Turbomix plus, Moulinex, France) to disrupt the cell walls and release

121 the cellular material. The resulting slurry was then filtered through a layer of cheesecloth to remove
122 the external part of the seeds (solid residues) and cell wall components. The filtrate corresponded to
123 the hemp seeds aqueous extract, which is called extract in this paper. Hemp seed extract is a natural
124 oil-in-water emulsion that contains OBs and plant storage proteins. In order to isolate OBs, hemp
125 seed extract was centrifuged at 1000 *g* for 30 min at 20°C (Eppendorf® 5810R centrifuge, Merck
126 KGaA, Darmstadt, Germany). The layer of OB-rich cream at the top of the tubes was manually
127 collected. The protein bodies were obtained as sedimented material after centrifugation of the hemp
128 seed extract at 4000 *g* for 30 min.

129 In an alternative to mechanical grinding, minimal processing was applied to the hydrated hemp
130 seeds: they were cutted with a knife, which induced the release of hemp seed components in the
131 aqueous phase.

132 **2.2.2. Homogenization**

133 The hemp seed extracts were passed through a two-stage laboratory high-pressure homogenizer
134 (PandaPlus 1000, GEA, Italy) at 40°C. Homogenization was performed at 10, 30 and 60 MPa. The
135 hemp seed extracts, without homogenization and after homogenization, were centrifuged at 4000 *g*
136 for 30 min to collect on the top the cream that was rich in natural OBs or homogenized OBs (noted H-
137 OBs) and on the bottom the pellet of sedimented proteins, in order to perform additional
138 characterizations (particle size measurements, confocal microscopy, chemical analysis). The non
139 homogenized and homogenized hemp seed extracts were stored at 4°C in order to characterize their
140 physical stability as a function of time.

141 **2.2.3. Changes in the pH and mineral environment**

142 The pH of OB suspensions was adjusted using 0.1 M HCl or NaOH solutions. Solutions of NaCl and
143 CaCl₂ were prepared by dissolving the required amount of the respective powders in ultrapure
144 (milliQ) water and adjusting the pH to 7.2. The OBs obtained by centrifugation were added to the
145 solutions to reach the final concentration of 8 wt% of lipids in the form of OBs. The samples have

146 been stored at room temperature for 4h and then stored at 4°C to follow their physical stability as a
147 function of time.

148

149 **2.3. Chemical analysis**

150 **2.3.1 Extraction and quantification of total lipids**

151 The lipid content of the whole hemp seeds was determined in triplicate by Soxhlet extraction with
152 petroleum ether as a solvent (Ntone et al., 2020). For the extraction of total lipids from the cream
153 concentrated in hemp seed OBs, the protocol of the cold extraction procedure developed by Folch
154 and collaborators was used (Folch et al., 1957). The quantification of total lipids from the OBs-rich
155 creams was performed in triplicate, from 3 independent experiments (n = 9). The lipid classes were
156 determined by high-performance thin-layer chromatography (HPTLC; CAMAG® HPTLC, Chromacim
157 SAS, Moirans, France) on silica plates (HPTLC Silica gel 60 F254 10x20 cm, 200 µm, Merck) with the
158 mixtures diethyl ether/acetone (80:20, v/v; on 3 cm) and then hexane/diethyl ether/acetic acid
159 (80:20:1, v/v/v), and revealed using copper sulfate (5 min, 100°C).

160 **2.3.2. Fatty acid profile of hemp seed OBs**

161 The fatty acid profile was determined by a gas chromatography (GC) procedure after methylation
162 with cold methanolic solution of potassium hydroxide. The fatty acid methyl esters (FAMES) were
163 analyzed by GC (Focus GC, Thermo Electron Corporation, Massachusetts, USA) equipped with a split
164 injector (ratio of 1/20), a CPCil 88 Varian capillary column (50 m × 0.25 mm with a 0.2-µm thick film;
165 Chrompack, Middelburg, The Netherlands) and 1 mL/min of helium as carrier gas. FAME were
166 analyzed using a flame ionization detector and ChromCard Data System (version 2005; Thermo
167 Electron Corporation, Massachusetts, USA). The FAME were identified using a mixture of methyl
168 esters as external standard (Mixture ME 100, Larodan, Sweden). The GC analysis was performed in
169 triplicate for each Folch extract of total lipids from hemp seed OBs.

170 **2.3.3. Quantification of total and individual sterols and sterol esters**

171 The identification and quantification of sterol esters was performed after fractionation of the Folch
172 extracts according to (ISO-8420, 2002) to recover the apolar fraction, and then according to (ISO-
173 122228-1, 2014). For the identification and quantification of total sterols, saponification of hemp
174 seed OBs Folch extract was performed with 15% KOH ethanolic solution, during 22 h in the dark at
175 room temperature. Then, deionized water and n-hexane were added and vigorously mixing on a
176 vortex. After separation of phases, the n-hexane fraction was evaporated under nitrogen stream until
177 dryness. The dried unsaponified material was derivatized with 100 μ L of silylating agent (Sylon HT Kit)
178 for 2 h in the dark at room temperature. After that, the reagent was evaporated under nitrogen
179 stream and the residue was dissolved in 1.0 mL of n-hexane. The solution was subjected to
180 centrifugation at 5,000 *g* for 5 min, and the upper phase was then transferred into vials suitable for
181 gas chromatography with flame ionization (GC-FID) analysis. A GC-2010 gas chromatograph equipped
182 with a split/splitless injector and a flame ionization detector (Shimadzu, Kyoto, Japan) was used with
183 a capillary silica column DB (60 m x 0.25 mm x 0.25 μ m; Varian). The different phytosterols were
184 identified by comparing the retention times with the individual standards (Sigma-Aldrich). The
185 internal standard 5α -cholestan- 3β -ol (Sigma D6128) was employed to quantification, by the ratio
186 between the concentration and peak areas of phytosterols and internal standard.

187 **2.3.4. Quantification of total and individual carotenoids**

188 The identification and quantification of the carotenoids was performed as in (NF-EN-12823-2, 2001).
189 The saponification of hemp seed OBs Folch extract was performed as for sterol analysis. The
190 carotenoids were extracted from the KOH/ methanolic phase and were analysed by HPLC (column
191 C18 Vydac 250 x 4mm) in isocratic conditions and detected at 450 nm. The individual carotenoids
192 were identified by using external standards. For quantification, the external standard beta-carotene
193 (Sigma-Aldrich) was used.

194 **2.3.5. Quantification of total and individual tocopherols and tocotrienols**

195 The quantification of total and individual tocopherols and tocotrienols was performed on Folch
196 extracts according to (ISO 9936:2016). Tocopherols standards (purity > 95%) were provided by Sigma-

197 Aldrich (St. Louis, MO). HPLC analysis was performed using the 1290 Agilent System (Massy, France)
198 equipped with a C18 column (250 mm × 4.6 mm i.d., 5 µm, HALO(R)-5 column, AMT, Wilmington,
199 Delaware, USA) and a fluorescence detector (296 nm for excitation and 330 nm for emission). The
200 mobile phase consisted of ethanol/methanol (40:60 v/v) in isocratic conditions. The temperature of
201 the column was maintained at 25°C and the flow rate was 0.8 mL/min. Each sample was analyzed in
202 triplicate.

203 **2.3.6. Polar lipid analysis of hemp seed OBs**

204 The quantification of total phospholipids and the determination of the individual phospholipid
205 classes in hemp seed OB samples were performed using HPLC combined with an evaporative light
206 scattering detector as previously described (Lopez et al., 2014). The identification of the
207 phospholipids was carried out by a comparison with the retention time of pure standards.
208 Quantitafication was performed using calibration curves.

209 **2.3.7. Protein quantification**

210 The determination of the protein content was carried out by spectrophotometric measurement using
211 a colored chemical reaction with bicinchoninique acid (BCA) according to Smith et al. (1985). BCA
212 Assay kit were from Uptima Interchim (Montluçon, France). Briefly, 25 µl of each sample were loaded
213 on microplate in triplicate and 200 µl of a mix of Reagent A and B was added. Bovin Serum Albumin
214 (BSA ; 2 mg/mL) with different dilutions (0 µg to 1000 µg) was used for calibration curve. After
215 incubation at 37°C for 30 min, the reading of the microplate was performed at 562 nm on microplate
216 spectrophotometer (Epoch, Biotek Instruments, France). Concentration of proteins was determined
217 after calculation from BSA standard curve taking into account the dilution factors of each sample.

218 **2.3.8. Gel electrophoresis**

219 **2.3.8.1 Preparation of the samples before gel electrophoresis**

220 The hemp seed extracts, without homogenization and after homogenization at 10, 30 and 60 MPa,
221 were centrifuged at 4000g for 30 min to recover the cream (top), the intermediate supernatant
222 aqueous phase and the sedimented centrifugation pellet (bottom).

223 For the determination of the interfacial protein composition of native OBs or homogenized OBs (H-
224 OBs) by gel electrophoresis, OBs and H-OBs were isolated from the aqueous phase to remove un-
225 adsorbed proteins from the interface according to a method adapted from Patton and Huston
226 (1986). Briefly, 10 g of the creams were mixed with 10 g of a solution containing containing 50% w/w
227 of sucrose. Then, in 50 mL plastic centrifuge tubes, 20 g of the treated hemp seed extract were
228 delivered under 30 g of a solution containing 5% w/w of sucrose. The tubes were centrifuged at
229 4000g for 30 min in order to form a layer of washed OBs or H-OBs at the top of the tubes.

230 **2.3.8.2 Gel electrophoresis**

231 The proteins contained in all the samples used for gel electrophoresis were quantified by BCA Assay
232 and the protein composition was characterized by SDS-PAGE with Mini-Protean TGX Precast Gels
233 12% using Mini-Protean Tetra Cell system (Bio-Rad Life Science, France). All reagents are from Bio-
234 Rad Life Science. The different protein samples were diluted in denaturing and reducing buffer.
235 Samples were diluted in 2x Laemmli sample buffer in reducing conditions with 2-mercaptoethanol
236 5% (a reducing agent that breaks down the disulfide linkages). The migration buffer contained 25
237 mM Tris, 192 mM glycine, 0.1% SDS according to Laemmli (1970) protocol. The samples were heated
238 at 100°C for 5 min. Each protein sample was then loaded on a sample well (20 µg of protein/well) of
239 the 12% polyacrylamide gel electrophoresis. Molecular weight (MW) protein markers from MW 3 to
240 198 kDa (SeeBlue Pre-stained Protein Standard, Novex Thermo Scientific, Les Ulis, France) and from
241 MW 14.4 to 116 kDa (unstained Molecular weight marker, Euromedex, Souffelweyersheim, France)
242 were used for MW calibration. The migration was carried out at 150 V for 45 min. The gel was
243 stained with Coomassie Brilliant Blue G-250 staining solution for 2h with gentle agitation on platform
244 rocker according to Lawrence and Besir (2009). The gel was rinsed with distilled water before
245 scanning on a flatbed scanner (Image Scanner iii, GE Healthcare, Souffelweyersheim, France).

246

247 **2.4. Physico-chemical characterisations**

248 **2.4.1. Particle size measurements**

249 The size distributions of OBs and protein bodies (PBs) were determined by using a laser diffraction
250 analyzer (Horiba LA-960V2, Retsch Technology, Germany). The refractive indexes used were 1.47 for
251 the OBs, 1.45 for the proteins, and 1.33 for the continuous phase (water). For measurements, the
252 samples were diluted as appropriate in ultrapure water. The particle size measurements of each
253 sample were performed at room temperature and in triplicate using three different samples.

254 **2.4.2. Zeta potential measurements**

255 Dispersions of OBs were diluted in solutions of various pHs or containing various amounts of NaCl or
256 CaCl₂ (100 µl OB dispersion in 10 mL solution). Diluted OB dispersions were filled into a cuvette,
257 which was then placed into the chamber of a Zetasizer Nano ZS (Malvern, Germany). The zeta
258 potential was calculated from the electrophoretic mobility of the OBs according to the Smoluchowski
259 approximation and Henry's law. The measurements were run five times at 25°C on at least three
260 independent and freshly prepared samples.

261

262 **2.5. Microstructure**

263 The microstructures of hemp seed extracts and OBs were examined by confocal laser scanning
264 microscopy (CLSM) using a microscope NIKON A1R (NIKON, Champigny sur Marne, France) with a x60
265 oil immersion objective. The lipid-soluble Nile Red fluorescent probe (5H-benzo-alpha-phenoxazine-
266 5-one,9-diethylamino; supplied by Sigma Aldrich, St Louis, USA; 100 µg/mL in propanediol) was used
267 to stain the TAG (excitation wavelength = 560 nm). Fast Green FCF (Sigma-Aldrich, St. Louis, USA ; 10
268 mg/mL in water) was used to stain proteins (excitation wavelength = 636 nm). The fluorescent head
269 group-labelled phospholipid analogue Lissamine rhodamine B sulfonyl
270 dioleoylphosphatidylethanolamine (Rh-DOPE, 1 mg/mL; Avanti Polar lipids Inc., Birmingham,
271 England) was used to characterize the hydrated hemp seeds and to investigate the lateral
272 distribution of phospholipids on the surface of OBs (excitation wavelength = 560 nm). The samples
273 were kept at room temperature for at least 30 min prior to observation by CLSM.

274

275 3. Results and discussion

276

277 3.1. Lipid composition of hemp seed OBs

278 The hemp seeds used in this study contained 33.6 ± 0.5 g of total lipids / 100 g of seeds, which was in
279 accordance with information given by the seed producer and with data found in literature (Farinon et
280 al., 2020). The lipid composition of the hemp seed OBs obtained by aqueous extraction and
281 centrifugation is presented in **Figures 1 and 2**. The schematic representation of a hemp seed OB
282 proposed **Figure 1-A** illustrates the localisation of the main components. As expected, lipid class
283 analyses confirmed the main amount of triacylglycerols (TAG ~ 95% of lipids; **Fig 1-B**), and the
284 presence of diacylglycerols, free fatty acids, phytosterols, tocopherols, carotenoids, and
285 phospholipids in hemp seed OBs. The fatty acid (FA) profile of hemp seed OBs showed that linoleic
286 acid (C18:2 *n*-6 ; LA), α -linolenic acid (C18:3 *n*-3 ; ALA) and oleic acid (C18:1 *n*-9) were the most
287 abundant FAs which together comprised 84.1% of the total FAs (**Fig 1-C**). The PUFAs of the oil
288 amounted to 72.9% of the total of FAs while the monounsaturated and saturated FAs amounted to
289 13.6 wt% and 9.2 wt%, respectively. The hemp seed OBs deliver the essential PUFAs *n*-6 and *n*-3 in
290 the proportion 3:1 that is the best ratio recommended by medical research and the most advanced
291 theories in the field of nutrition. Our results on the FA composition of hemp seed OBs were in
292 agreement with literature on hemp seeds and oil (Farinon et al., 2020; Montserrat-de la Paz et al.,
293 2014).

294 Hemp seed OBs contained 206 ± 7 mg phospholipids / 100 g lipids (0.21 wt%). The relative
295 proportion of the individual OBs phospholipids is presented **Figure 1-D**. The main phospholipids of
296 hemp seed OBs were the zwitterionic phosphatidylcholine species (PC ; 32.3 wt% PL), in agreement
297 with literature (Antonelli et al., 2020). The zwitterionic phosphatidylethanolamine (PE) accounted for
298 11.3%wt of total phospholipids. The anionic phospholipids phosphatidylserine (PS ; 10.1 wt% PL) and
299 phosphatidylinositol (PI ; 12.5 wt% PL) were also detected, in agreement with literature (Furse et al.,

2013; Tzen et al., 1993). Phosphatidic acid (PA) accounted for 30.4 wt% PL. Altogether, the anionic phospholipids (sum of PS, PI and PA) accounted for 53 wt% of total phospholipids.

The unsaponifiable fraction of hemp seed OBs contained carotenoids (**Fig 2-A**), tocopherols (**Fig 2-B**) and phytosterols (**Fig 2-C**). The carotenoids accounted for 8.3 ± 0.3 mg/100 g lipids (2.8 mg/100 g hemp seeds), with the three main carotenoids being lutein (80 wt% carotenoids ; 6.6 ± 0.2 mg/100 g lipids; 2.2 mg/100 g hemp seeds), beta-carotene and zeaxanthin, in agreement with literature (Farinon et al., 2020). The sum of tocopherols and tocotrienols accounted for 84.4 ± 0.8 mg / 100 g of lipids. The tocopherol profile revealed that γ -tocopherol was the most abundant isomer, i.e. 96.7 wt% of total tocopherols, in agreement with literature on hemp (Farinon et al., 2020; Montserrat-de la Paz et al., 2014). Natural fat-soluble functional compounds with high antioxidative activity such as the tocopherols are therefore intrinsically associated to hemp seed OBs. The phytosterol amount was 341.5 ± 3.6 mg / 100 g of lipids. The main phytosterols characterised in hemp seed OBs were β -sitosterol (67 wt% sterols; 228 mg/100 g of lipids), campesterol, δ 5-avenasterol and stigmasterol, which is in agreement with literature (Farinon et al., 2020; Montserrat-de la Paz et al., 2014). The sterols in the esterified form corresponded to about 50 wt% of total sterols (**Fig. 2-C**).

315

316 **3.2. Microstructure**

317 **Figure 3** shows the microstructure of hydrated hemp seeds, hemp seed extracts and OBs. At the
318 microscopic level, and according to their size, mainly the OBs and the PBs were observed. Within the
319 hydrated hemp seeds, the OBs and the PBs appeared closely packed with OBs filling the space
320 between PBs. Both the OBs and the PBs exhibited a spherical shape, with a larger size observed for
321 PBs compared to OBs (**Fig 3-A**), in agreement with observations of peanut seeds and soybean
322 cotyledon (Nikiforidis et al., 2014; Zaaboul et al., 2018). The specific labelling of phospholipids
323 revealed their localisation in membranes within the seed and around the OBs (**Fig 3-A3**).

324 The mechanical processes applied to the hydrated seeds induced the release of individual OBs and
325 PBs, both of spherical shape, as well as other soluble components and their homogeneous dispersion

326 in the aqueous extract. Hemp seed extract is therefore a natural oil-in-water emulsion and a
327 dispersion of proteins (**Fig 3-B**). The size distributions of the hemp seed OBs and PBs determined by
328 laser light scattering were monomodal and ranged from 0.3 to 8 μm for OBs and from 1.3 to 20 μm
329 for PBs (**Fig 3-B**). The volume-averaged diameters of hemp seed OBs and PBs were $2.3 \pm 0.1 \mu\text{m}$ and
330 $4.1 \pm 0.3 \mu\text{m}$, respectively. This is in accordance with the size of OBs reported in literature. The
331 volume-averaged diameters of sesame and peanut OBs were reported to be $2.4 \pm 0.4 \mu\text{m}$ and $2.3 \pm$
332 $0.3 \mu\text{m}$ respectively, with sizes ranging from 1 to 10 μm (Yang et al., 2020). The similar OB sizes
333 observed by CLSM inside the seeds (**Fig 3-A**) and after the aqueous extraction by grinding (**Fig 3-B**)
334 indicated that the hemp seed OBs have not been mechanically disrupted during preparation.

335 The hemp seed OBs showed a large core region rich in TAG (**Fig 3-C**). CLSM images of hemp seed OBs
336 revealed non-fluorescent areas in the core of OBs. They were located at the periphery of OBs and
337 absent from the internal core of the OBs, as revealed by observations at different z-depths (**Fig 3-C1**).
338 According to previous observations reported in literature (Czabany et al., 2008), the structures
339 revealed by CLSM could correspond to steryl esters in an ordered state that segregated from the
340 fluid TAG phase.

341 CLSM observations showed a heterogeneous distribution of proteins at the surface of hemp seed
342 OBs (**Fig 3-C**). These proteins located at the surface of native OBs could correspond to the specific
343 membrane-associated proteins described for OBs (oleosins, caleosins and steroleosin; **Fig. 1-A**)
344 (Nikiforidis et al., 2014; Tzen et al., 1993).

345 The monolayer of phospholipids on the OB surface, that delimit their hydrophobic TAG core, was
346 investigated (**Fig 3-D**) and revealed areas in which the Rh-DOPE fluorescent dye was not able to
347 integrate (**Fig 3-D3**). These areas could correspond to the concentration of proteins embedded in the
348 fluid matrix of phospholipids (i.e. oleosins, caleosins and steroleosin) or to ordered domains formed
349 for example by sterols in the plane of the phospholipid monolayer. The heterogeneous distributions
350 of proteins and phospholipids at the surface of hemp seed OBs that have been observed in this study

351 contrast with the uniform layers of proteins and phospholipids reported on the surface of OBs from
352 almond milk and coconut milk (Dave et al., 2019; Gallier et al., 2012).

353

354 **3.3. Homogenization to improve the physical stability of hemp seed extracts**

355 The physical stability of hemp seed extracts as a function of time and the impact of high-pressure
356 homogenization were investigated (**Figures 4 and 5**). Freshly prepared hemp seed extracts showed
357 spontaneous phase separation within a few hours with partitioning into a sedimented layer, a milk-
358 white phase and a top cream layer (**Fig. 4-C**). A technological process able to decrease the size of the
359 particles and avoid phase separation upon long-time storage is high-pressure homogenization. Hemp
360 seed extracts were therefore submitted to homogenization under various pressures ranging from 0
361 to 60 MPa. CLSM observations of the hemp seed extracts showed the coexistence of OBs with a
362 decrease in their size as a function of the increase in the homogenization pressure, and large
363 spherical PBs (**Fig 4-A**). Some OBs were in interaction with PBs after homogenization (**Fig 4-A, insert**).
364 The size distributions of the non-homogenized and homogenized hemp seed extracts, as well as the
365 size distributions of the OBs and PBs that have been selectively separated from the homogenized
366 samples by centrifugation, are presented **Figure 4-B**. High-pressure homogenization successfully
367 decreased the diameter of hemp seed OBs while it induced a small reduction in the diameter of the
368 PBs (**Fig. 4-B5**). The mean diameter of OBs decreased from 2.3 μm (size range: 0.3 to 8 μm) to 0.26
369 μm (size range: 0.08 to 0.8 μm) after homogenization at 60 MPa. The mean diameter of PBs
370 decreased from 4 μm (size range: 1.3 to 20 μm) to 2.6 μm (size range: 0.9 to 6 μm ; 60 MPa).

371 Further chemical and microscopic observations were performed in order to identify the components
372 in the sedimented material and in the top cream layer (**Fig. 5**). Gel electrophoresis showed that the
373 globulin edestin, including its acidic sub-units (33 kDa) and basic sub-units (20 kDa), was the major
374 protein of the hemp seed extracts in accordance with literature (Malomo et al., 2014; Tang et al.,
375 2006). The protein 7S globulin (48 kDa) and the water-soluble albumins (below 20 kDa) were also
376 detected. The sedimented material (pellet after centrifugation) was mainly composed of edestin

377 while the supernatant contained water-soluble proteins. Similar results were obtained for
378 unhomogenized and homogenized hemp seed extracts (**Fig. 5-A**). The globulin edestin was recovered
379 in the sedimented material as a consequence of its higher density than the density of water (density
380 of PBs from seeds around 1.3 ; (Tully and Beevers, 1976)) and low solubility in water since edestin is a
381 salt-soluble globulin. Indeed, the globulin edestin requires high ionic strength solvents to be
382 solubilised, for example sodium phosphate/sodium chloride buffer at pH 7.8 with a ionic strength of
383 500 mM (St Angelo et al., 1968). The top cream layer was rich in OBs, as a result of their low density
384 in comparison to water. The proteins adsorbed at the surface of natural and homogenized OBs were
385 identified. As expected (**Fig. 1-A**), oleosins isoforms (15 – 20 kDa), caleosin (35 kDa) and steroleosin
386 (50 kDa) were identified as interfacial proteins of the natural OBs (**Fig. 5-A**). Increasing the
387 homogenization pressure induced changes in the interfacial protein composition of the H-OBs, with
388 an increased relative proportion of edestin, as shown by the presence of its acidic sub-units (33 kDa)
389 and basic sub-units (20 kDa). These results showed that the increase in the OBs surface area
390 associated to the decrease in their size as a function of the homogenization pressure applied induced
391 the adsorption of edestin to stabilize the interface created upon homogenization. Interestingly, gel
392 electrophoresis showed the presence of oleosin isoforms at the surface of H-OBs even after
393 homogenization at 60 MPa (**Fig. 5-A**).

394 CLSM observations showed that, in absence of homogenization, the top layer formed as a function
395 of time or obtained after centrifugation was enriched in natural OBs of larger size than in the
396 supernatant while the sedimented material or pellet obtained after centrifugation corresponded
397 mainly to PBs characterized by their spherical shape, e.g hemp seed's globulin edestin (**Fig. 5-B**). In
398 the samples homogenized at 10 MPa, the sedimented material was composed of PBs alone, and of
399 complexes formed between PBs and OBs of small size induced by homogenization as shown by CLSM
400 (**Fig. 5-B6**). The density of the PBs-OBs complexes depends on the relative proportion of lipids and
401 proteins (such as for lipoproteins). The large size, low solubility in water and high density of the
402 hemp seed PBs associated with the small size and low density of the H-OBs induced the

403 sedimentation of the PBs-OBs complexes. In the samples homogenized at 10 MPa, the top cream
404 layer contained small particles of proteins in interaction with the homogenized OBs, as shown in **Fig.**
405 **5-B4**. The adsorption of water-insoluble particles of hemp seed proteins, mainly the colloidal PBs
406 composed of edestin, at the surface of homogenized OBs opens perspectives for their potential
407 utilization as stabilizers in food-grade Pickering emulsions (Sarkar and Dickinson, 2020).

408 As a conclusion, the homogenization process induced a physical stabilization of the hemp seed OBs
409 for homogenization pressures above 10 MPa by reducing their size below 1 μm (**Fig. 4-B**) but the
410 large PBs sedimented as a consequence of their size larger than 1 μm , their poor water solubility and
411 their high density (**Fig 4-C; Fig. 5**). The impact of high-pressure homogenization that affects both the
412 composition and the architecture of the natural OBs surface, on the oxidative alteration of OBs PUFA
413 will be further investigated by our group.

414

415 **3.4. Impact of pH and minerals on the surface properties of OBs and physical stability of** 416 **the emulsions**

417

418 **3.4.1. Impact of pH**

419 The ζ -potential values of hemp seed OBs, obtained either by minimal mechanical processing or by
420 mechanical grinding of the hydrated hemp seeds, were determined as a function of pH (**Fig 6**). The
421 mechanical treatments used during aqueous extraction of the hemp seed OBs did not significantly
422 affect the ζ -potential values measured as a function of pH, indicating an absence of changes or
423 alteration of the surface properties of the OBs. The ζ -potential of the OBs decreased from negative to
424 positive with decreasing pH (**Fig 6-A**). Above $\text{pH} \geq 9$, the ζ -potentials of the OBs reached a plateau
425 with $\zeta = -55$ mV. The absolute values of ζ -potential measured for hemp seed OBs decreased with pH
426 until reaching the isoelectric point (IEP ; $\zeta = 0$ mV) in the range $\text{pH} 4.4 - 4.6$ (**Fig 6-A**). For pHs below
427 the IEP, the ζ -potential values were positive, with $\zeta = +40$ mV below pH3. This is in agreement with
428 previous studies reporting that the ζ -potential of maize OBs ranged from -40 mV at pH 7 to +35 mV at

429 pH 3 (Nikiforidis and Kiosseoglou, 2009). The ζ -potentials of sesame OBs, peanut OBs, sunflower OBs
430 and soybean OBs have been reported to follow similar trends ranging from -25 to -35 mV at pH 8 to
431 +25 mV at pH 2 (Wang et al., 2019; Yang et al., 2020). The IEP found in this study for hemp seed OBs
432 is in agreement with the zero charge point reported between pH 4.5 and pH 5 for maize OBs
433 (Nikiforidis and Kiosseoglou, 2009), as well as for sesame, soybean, sunflower and peanut OBs (Qi et
434 al., 2017; Wang et al., 2019; Yang et al., 2020).

435

436 The physical stability of the emulsions containing hemp seed OBs was examined as a function of pH
437 and combined with structural observations performed by confocal microscopy (**Fig 6 B & C**). Changes
438 in pH affected the physical stability of the hemp seed OBs. For pH values above pH 7.5, the OBs in
439 water emulsions were physically stable, in accordance with strong electrostatic repulsions due to the
440 negative charge of the OBs at this pH (-30 to -55 mV; **Fig. 6-A**). For $3.3 \leq \text{pH} \leq 7.1$, a layer
441 concentrated in OBs was rapidly formed at the top of the samples (**Fig. 6-B**). The bottom of the
442 samples was turbid from pH 5.5 up to pH 7.1 while it was clear for $3.3 \leq \text{pH} \leq 5.8$. In this range of
443 pHs, CLSM observations revealed the formation of OBs aggregates (**Fig. 6-C**). At pH 6.2, small OBs
444 aggregates were observed. The sizes of the OBs aggregates were larger below pH 6. CLSM images
445 showed that the proteins corresponding mainly to oleosins located at the surface of OBs were
446 involved in the formation of the OBs aggregates. For pHs ranging from 5.0 to 4.5, that correspond
447 to the IEP of hemp seed OBs (**Fig. 6-A**), large aggregates of OBs connected by proteins were observed
448 together with the formation of large OBs formed by coalescence. For pH 3.7 and 3.3, large particles
449 containing aggregated proteins originating from OBs surface and non-spherical oil droplets
450 coalescing at their periphery were observed (**Fig 6-C**). For pH 2.9, the whole content of the tube was
451 turbid and the samples did not show phase separation at the macroscopic level (**Fig 6-B**), while CLSM
452 observations showed the formation of small aggregates of OBs (**Fig 6-C**).

453 Our results on the impact of pH are in agreement with previous reports on OBs from other plant
454 sources. Extensive aggregation of sunflower-seed OBs was reported between pH 5 and 6 (around the

455 IEP), without coalescence, and associated to a high creaming (White et al., 2008). OBs isolated from
456 maize maintained their entities at pH 7.2 but aggregated when the pH was lowered to 6.8 and 6.2
457 (Tzen et al., 1992).

458 The composition and structure of the hemp seed OBs surface governed their sensitivity to pH and the
459 physical stability of the emulsion. The overall electronegative charge of hemp seed OBs surface at
460 neutral pH results from i) the presence of charged phospholipids (anionic and containing a negatively
461 charged phosphate group such as PA or within neutral phospholipids such as PC; **Fig 1**), and ii) the
462 topology of the oleosins (main OB-associated proteins) in the OB membrane that expose their
463 negatively charged residues (i.e. the acidic amino acids in the N- and C-termini) to the aqueous phase
464 (Huang, 1994). These negative charges of OBs were responsible for electrostatic repulsions and
465 physical stability of the OBs-in-water emulsions towards aggregation. Decreasing the pH, i.e.
466 increasing the amount of protons H^+ in the aqueous phase surrounding the OBs, decreased the
467 electrostatic repulsions between OBs. The overall charge of the OBs was insufficient to generate
468 repulsive forces greater than the attractive interactions, hydrophobic and Van der Waals, that were
469 present between the OBs, resulting in OBs aggregation. OBs aggregates of large size phase separated
470 from the aqueous phase and reached the top of the samples due to the low density of oil. Authors
471 reported that the IEP of intrinsic oleosin proteins associated with the surface of the OBs is comprised
472 between pH 5 and 6 (White et al., 2008). When the pH of OBs in water emulsion was close to the IEP
473 of these stabilizing proteins, OBs aggregation occurred. The low amount of coalescence of OBs for pH
474 above IEP has been attributed to steric hindrance (Tzen and Huang, 1992; Tzen et al., 1992), but also
475 to the strength of the natural emulsifying layer of OBs due to the association between the N- and C-
476 termini of the oleosin protein with the phospholipids preventing closely associated OBs from losing
477 their integrity (White et al., 2008). The pKa of the charged groups of the phospholipids should also be
478 considered to explain the impact of pH on the hemp seed OBs. The COOH group of the anionic
479 phospholipid PS exhibits a pKa close to 5.5 and the pKa of the phosphate group of the phospholipids
480 is close to pH 3 (Marsh, 2013), which means that the negative charge no longer exist below these key

481 pH values. Changes in pH affected the individual molecules present at the surface of OBs
482 (phospholipids and proteins) but also possibly the proteins - phospholipids interactions and the
483 conformation of the proteins in the OB hemi-membrane (changes in the exposure of protein
484 hydrophobic regions to the aqueous phase) (Qi et al., 2017).

485 The impact of pH on the physical stability of hemp seed OBs that leads to aggregation and
486 coalescence should be considered in the formulation of foods, for exemple acidic products such as
487 fermented products and mayonnaise.

488

489 **3.4.2. Impact of NaCl and CaCl₂**

490 The impact of monovalent (Na⁺) and divalent (Ca²⁺) ions on the negatively charged surface of hemp
491 seed OBs was examined at pH 7.2. These cations were provided by NaCl and CaCl₂, respectively.

492 In a first set of experiments, hemp seed OBs were dispersed in presence of various amounts of NaCl,
493 with concentrations varying from 0 to 500 mM (8 wt% OBs in the samples) (**Fig 7**). Changes in the ζ -
494 potential values as a function of the concentration in NaCl are presented **Figure 7-A**. The ζ -potential
495 of OBs decreased quite linearly from $\zeta = -29.8 \pm 2.2$ mV in absence of NaCl to $\zeta = -9.8 \pm 1.1$ mV in
496 presence of 50 mM NaCl, and decreased to a lesser extend for high concentrations in NaCl ($\zeta = -2.8$
497 ± 2.4 mV for 500 mM NaCl). Macroscopic observations revealed a physical instability of the hemp
498 seed OBs induced by NaCl, with the formation of a OB-rich cream layer at the surface of the tubes
499 mainly for concentrations ranging from 20 to 100 mM NaCl (**Fig 7-B**). This was related to the
500 aggregation of hemp seed OBs in presence of NaCl induced by the decrease in the electrostatic
501 repulsions as a result a low zeta potential values. The thickness of the OB-rich cream layer was
502 smaller for NaCl amounts of 200 and 500 mM compared to the range 20 to 100 mM NaCl. This could
503 be attributed to structural reorganisations of interfacial proteins in presence of high amount of NaCl,
504 with steric repulsions between hemp seed OBs. Below the OB-rich cream layer, the turbidity of the
505 samples was high whatever the amount of NaCl, indicating a high proportion of OBs dispersed in the
506 volume. CLSM observations of the samples showed the formation of OB aggregates in presence of

507 NaCl, with a connectivity between the surface layer of several OBs (**Fig 7-C**). In this study, we showed
508 that NaCl affects the surface properties of OBs components, probably both phospholipids and
509 proteins, with a decrease in ζ -potential values leading to a reduction of repulsive interactions and
510 then to an aggregation of OBs. Large OBs aggregates raised at the surface of the samples and formed
511 the OB-rich cream layer. From the CLSM images, we concluded that NaCl did not induce coalescence
512 of the hemp seed OBs. Our results are in agreement with authors who reported aggregation of OBs
513 from maize at pH 7.2 in presence of NaCl (10 – 1000 mM ; -5 to -20% turbidity) (Tzen et al., 1992).

514 In a second set of experiments, hemp seed OBs were dispersed in presence of various amounts of
515 CaCl_2 , with concentrations ranging from 0 to 10 mM (8 wt% OBs in the samples ; **Fig 8**). Changes in
516 the ζ -potential values as a function of the concentration in CaCl_2 are presented **Figure 8-A**. The ζ -
517 potential values decreased from $\zeta = -29.7 \pm 2.7$ mV in absence of CaCl_2 to $\zeta = -5.6 \pm 0.5$ mV in
518 presence of 2 mM CaCl_2 , and to $\zeta = -0.8 \pm 0.2$ mV in presence of 10 mM CaCl_2 . At pH 7.2, e.g. above
519 the IEP of the OBs, the divalent cations Ca^{2+} were the main counter-ions. They were therefore
520 involved in the reduction of the ζ -potential values measured as a function of the increase in CaCl_2
521 concentration in the OB dispersions. These experiments showed the ability of Ca^{2+} ions to associate
522 with the negatively charged OBs surface composed of membrane-associated proteins and
523 phospholipids (**Fig. 1-A**). At the macroscopic level, the physical instability of the hemp seed OBs
524 leading to creaming was induced by low concentration in CaCl_2 (**Fig 8-B**). A OB-rich cream layer was
525 rapidly observed in presence of $[\text{CaCl}_2] \geq 0.4$ mM, which corresponded to ζ -potential values below -
526 10 mV. For $[\text{CaCl}_2] \geq 2$ mM, the turbidity of the samples below the OB-rich cream layer was low,
527 indicating that most of the hemp seed OBs were concentrated in the cream layer. CLSM observations
528 revealed the formation of OB aggregates in presence of 0.2 mM CaCl_2 and above. For $[\text{CaCl}_2] \geq 4$ mM,
529 non-spherical and large lipid particles were observed within the OB aggregates. This was interpreted
530 as coalescence of hemp seed OBs (**Fig 8-C**). The impact of CaCl_2 on OBs aggregation found in our
531 study is in agreement with previous studies performed by other groups on other sources of OBs. An
532 aggregation of maize OBs was reported at pH 7.2 in presence of CaCl_2 above 1 mM (Tzen et al.,

533 1992), an aggregation of sunflower-seed OBs (emulsion, 10 wt%) was reported at pH 7 in presence of
534 CaCl_2 above 5 mM associated with an intensive creaming (White et al., 2008). Despite aggregation of
535 OBs has already been reported by several authors, the coalescence of OBs due to the presence of
536 calcium ions has not yet been described.

537

538 At neutral pH, cations such as H^+ , Na^+ and Ca^{2+} can interact with the negatively charged membrane-
539 associated proteins, and with the negative charge of phospholipids (anionic PS and PI ; phosphate
540 group of PC, PE and PA) present at the surface of hemp seed OBs (**Fig 1-A**). Our experiments showed
541 that the divalent cations Ca^{2+} interacted more strongly with the OB membrane components and had
542 a more important impact on the emulsion physical stability than the monovalent cations Na^+ (**Figure**
543 **7 & 8**). This is in agreement with Tzen's group who reported that aggregation of OBs from maize
544 could be induced with 2 mM CaCl_2 at pH 7.2, but not with NaCl suggesting that aggregation was due
545 to the association of divalent cations with the negatively charged OB surface (Tzen et al., 1992). The
546 divalent ions are more effective at screening electrostatic interactions and at binding to oppositely
547 charged groups (Israelachvili, 2011), leading to aggregation. Several molecular mechanisms, alone or
548 in combination, could underly the impact of low concentrations in Ca^{2+} ions on the surface properties
549 of OBs. First, Ca^{2+} ions could interact with the negative charges of the membrane-associated proteins
550 exposed to the aqueous phase, and affect the conformation of these proteins with consequences on
551 the surface hydrophobicity leading to OB aggregation. Specifically, Ca^{2+} could interact with the
552 calcium-binding caleosins tightly associated with OBs and may be involved in processes such as OB
553 aggregation and OB membrane fusion as previously reported by others (Naested et al., 2000;
554 Purkrtova et al., 2008). Caleosins on one OB surface may form Ca^{2+} -mediated associations with
555 caleosins located on an other OB surface, which would contribute in OB aggregation and membrane
556 fusion (Naested et al., 2000). Second, Ca^{2+} ions could affect the interactions between the negatively
557 charged phospholipids and the positively charged residues of the membrane-associated proteins
558 located at the surface of OBs. Third, Ca^{2+} ions could interact with the phospholipids through 3 binding

559 sites, i.e. the carboxylate groups (PS), phosphates (PS, PI, PC, PE, PA) and the carbonyl oxygen groups
560 of the phospholipid chains (Melcrová et al., 2016). The scientific literature describes the specific role
561 of Ca^{2+} ions in membrane fusion phenomena and particularly of membranes containing the anionic
562 polar head group PS, through the ability to form an anhydrous $\text{Ca}^{2+}(\text{PS})_2$ complex between apposed
563 phospholipid layers during initial aggregation (Wilschut et al., 1981). The fusion, that is defined as the
564 joining of two closely opposed lipid layers to form a single layer, involves the functional role of
565 specific lipids such as PS among the complex composition of natural membranes. The aggregation
566 and the subsequent coalescence of OBs could therefore involve OBs membrane fusion through the
567 action of Ca^{2+} ions on the anionic PS molecules located in the surface monolayer and that represent
568 10 ± 2 wt% of hemp seed OBs phospholipids as determined in our study (**Fig 1**). Deciphering the
569 Ca^{2+} -mediated mechanisms involved in OB membrane fusion would deserve to be further
570 investigated at the molecular level.

571

572 **4. Conclusions**

573 In this study, we successfully used minimal processing including aqueous extraction by grinding to
574 obtain aqueous dispersions containing hemp seed OBs and PBs. Chemical analyses showed that the
575 nutrient and bioactive compounds of hemp seed OBs, such as PUFA with an optimal n-6/n-3 ratio of
576 2.9, phospholipids, carotenoids with 80 wt% lutein, phytosterols with 67 wt% β -sitosterol, and γ -
577 tocopherols contribute to their nutritional interest and potentiel health benefits and encourage the
578 increased valorization of hemp seed OBs based food products in the human diet. We showed that
579 the size of natural hemp seed OBs and their naturally-occurring surface govern their physical stability.
580 Homogenization of hemp seed aqueous extracts was able to avoid phase separation of OBs for a long
581 time storage by reducing their size, but weakly reduced the size of the PBs that sedimented alone or
582 in interaction with homogenized OBs. We showed that stressful environmental conditions induced by
583 pH and minerals (NaCl and CaCl_2) to which they were exposed induced the physical unstability of
584 both the OBs and the emulsions. The results found in this study increased knowledge about the

585 chemical composition, surface properties and physical unstability of hemp seed OBs due to their size
586 and their ionic environment. This study will undoubtedly contribute in the economic valorization of
587 hemp seed OBs, in extending the range of novel food products containing hemp seed OBs and opens
588 perspectives for the development of hemp seed based emulsions.

589

590

591 **Acknowledgements**

592 Christelle Lopez thanks all the UR BIA's members involved in the "hemp project" for stimulating
593 discussions. The authors warmly thank Alain Riaublanc and Adeline Boire (INRAE, BIA, ISD, Nantes,
594 France) for interesting discussions about hemp seed proteins and protein bodies. Valérie Beaumal
595 and Elisabeth David-Briand (INRAE, BIA, ISD, Nantes, France) are acknowledged for help in particle
596 size and zeta potential measurements. Yann Gohon (Institut Jean-Pierre Bourgin, Versailles, France) is
597 acknowledged for interesting discussions about the partitioning of TAGs and steryl esters within the
598 core of oil bodies. Itegr (Canejan, France) is acknowledged for pertinent discussions about lipid
599 analyses.

600

601 **Declaration of competing interest**

602 The authors declare no conflict of interest.

603

604 **CRediT authorship contribution statement**

605 **Christelle Lopez:** Conceptualization, Supervision, Investigation, Writing – original draft and revision.

606 **Bruno Novales:** Conceptualization, Writing – original draft and revision.

607 **Hanitra Rabesona:** Conceptualization, Investigation, Writing.

608 **Magalie Weber:** Conceptualization, Writing – original draft and revision.

609 **Thierry Chardot:** Conceptualization, Writing – original draft and revision.

610 **Marc Anton:** Conceptualization, Writing – original draft and revision.

611

612 **Figure caption**

613 **Figure 1:** Lipid composition of hemp seed oil bodies. **(A)** Schematic representation of a hemp seed oil
614 body ; **(B)** Lipid classes ; **(C)** Fatty acids ; **(D)** Phospholipids. The chemical structures of the main
615 components are indicated in the figures. Abbreviations: MAG: monoacylglycerols, DAG:
616 diacylglycerols, TAG: triacylglycerols, FFA: free fatty acids, PL: phospholipids, PC :
617 phosphatidylcholine, LPC : lysophosphatidylcholine, PE : phosphatidylethanolamine, PA :
618 phosphatidic acid, PI : phosphatidylinositol, PS : phosphatidylserine.

619

620 **Figure 2:** Lipid composition of hemp seed oil bodies. **(A)** Carotenoids ; **(B)** Tocopherols and
621 tocotrienols, **(C)** Sterols, including total sterols and sterol esters.

622

623 **Figure 3:** Microstructure characterized by confocal laser scanning microscopy (CLSM). **(A)** Hemp
624 seeds containing protein bodies (PBs : green colour, fast green fluorescent dye) and oil bodies (OBs :
625 Red colour, Nile red fluorescent dye in A1 and A2, rhodamine-DOPE fluorescent dye in A3) , **(B)**
626 Dispersion of OBs and PBs obtained by aqueous extraction from hemp seeds observed by CLSM
627 (OBs : Red colour, Nile red fluorescent dye ; PBs : green colour, fast green fluorescent dye) and size
628 distributions characterized by laser light scattering; **(C)** Hemp seed OBs with the labelling of their
629 core rich in triacylglycerols (Red colour : Nile red fluorescent dye) and membrane-associated proteins
630 (green colour : fast green fluorescent dye) ; **(D)** Hemp seed OBs with the labelling of their monolayer
631 of phospholipids (red colour : rhodamine-DOPE fluorescent dye) and PBs (green colour, fast green
632 fluorescent dye).

633

634 **Figure 4:** Impact of high-pressure homogenization on hemp seed extracts : **(A)** microstructure of
635 hemp seed extracts as a function of the homogenization pressure applied with the labelling of the oil
636 bodies (OBs : Red colour, Nile red fluorescent dye) and the protein bodies (PBs : green colour, fast

637 green fluorescent dye) ; **(B)** Size distributions measured by laser light scattering; **(C)** physical stability
638 of hemp seed extracts as a function of the homogenization pressure applied.

639

640 **Figure 5:** Impact of high-pressure homogenization on hemp seed extracts : **(A) Left:** gel
641 electrophoresis showing the protein composition in the hemp seed extract (HSE), and in the
642 supernatant (Sup) and pellets obtained after centrifugation. The results are shown without
643 homogenization and after homogenization with the pressures indicated in the figure. **Right:** gel
644 electrophoresis showing the interfacial protein composition of natural OBs and homogenized OBs,
645 and the protein composition in the HSE without homogenization or after homogenization at 60 MPa.
646 **(B)** confocal laser scanning microscopy images showing the oil bodies (OBs : Red colour, Nile red
647 fluorescent dye) and the protein bodies (PBs : green colour, Fast green fluorescent dye) in the top
648 cream layer, the supernatant and the pellet obtained after centrifugation as indicated in the figure.

649

650 **Figure 6:** Impact of pH on hemp seed oil bodies (OBs) dispersions obtained by aqueous extraction.
651 **(A)** Zeta-potential of the OBs as a function of pH. The OBs were obtained either by grinding or by
652 minimal processing as indicated in the figure; **(B)** physical instability of OB dispersions as a function of
653 pH ; **(C)** confocal laser scanning microscopy images of OB dispersions as a function of pH, the core
654 rich in triacylglycerols was stained with Nile red (red colour) and the proteins located at the surface of
655 the oil bodies were stained with Fast Green FCF (green colour) fluorescent dyes. The scale bars
656 correspond to 10 μm . The arrows indicate coalescence of OBs at the periphery of OB aggregates.

657

658 **Figure 7:** Impact of sodium chloride (NaCl) on hemp seed oil bodies (OBs) dispersions obtained by
659 aqueous extraction. **(A)** Zeta-potential of OBs as a function of NaCl concentration. **(B)** physical
660 stability of OB dispersions as a function of NaCl concentration as indicated in the figure. **(C)** Confocal
661 laser scanning microscopy images of OB dispersions in presence of various amounts of NaCl as
662 indicated in the figure (samples from figure B); the hydrophobic lipid core of OBs was stained with

663 Nile red fluorescent dye (red colour) and the proteins were stained with fast green FCF fluorescent
664 dye (green colour). Scale bars correspond to 10 μm .

665

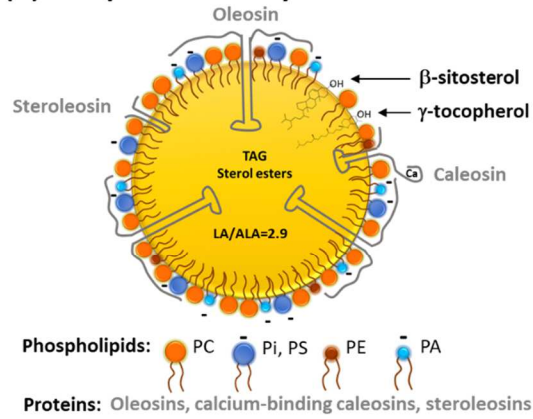
666 **Figure 8:** Impact of calcium chloride (CaCl_2) on hemp seed oil bodies (OBs) dispersions obtained by
667 aqueous extraction. **(A)** Zeta-potential of OBs as a function of CaCl_2 concentration. **(B)** physical
668 stability of OB dispersions as a function of CaCl_2 concentration as indicated in the figure. **(C)** Confocal
669 laser scanning microscopy images of OB dispersions in presence of various amounts of CaCl_2 as
670 indicated in the figure (samples from figure B); the hydrophobic lipid core of OBs was stained with
671 Nile red fluorescent dye (red colour) and the proteins were stained with fast green FCF fluorescent
672 dye (green colour). Scale bars correspond to 10 μm .

673

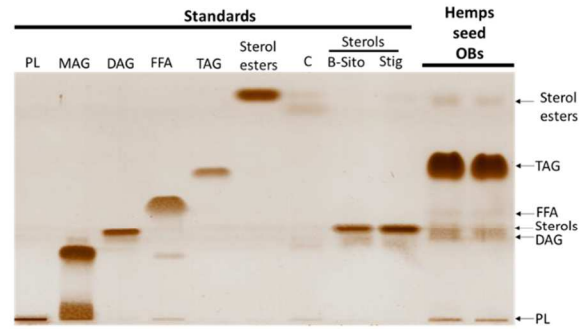
674 **FIGURES**

675 **Figure 1**

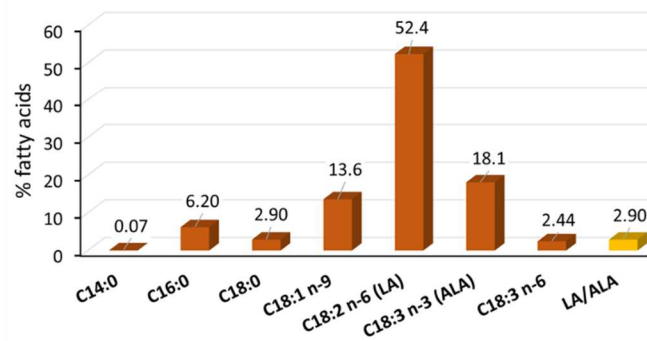
(A) Hemp seed oil body



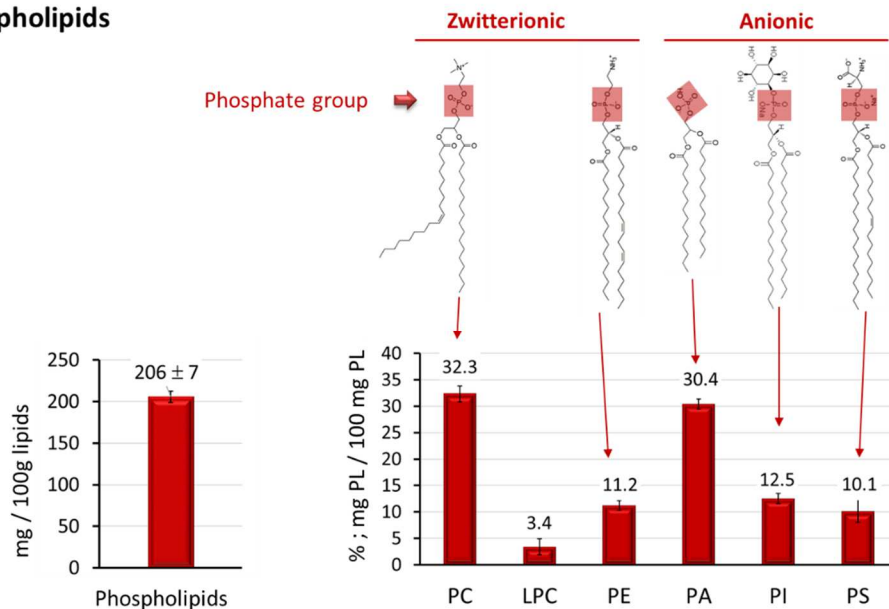
(B) Lipid classes



(C) Fatty acids



(D) Phospholipids



676

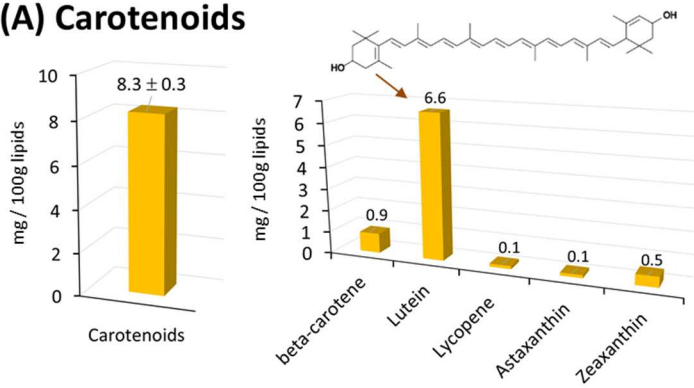
677

678

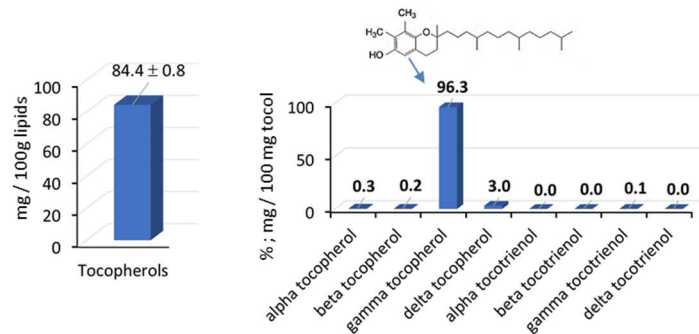
679

680 **Figure 2**

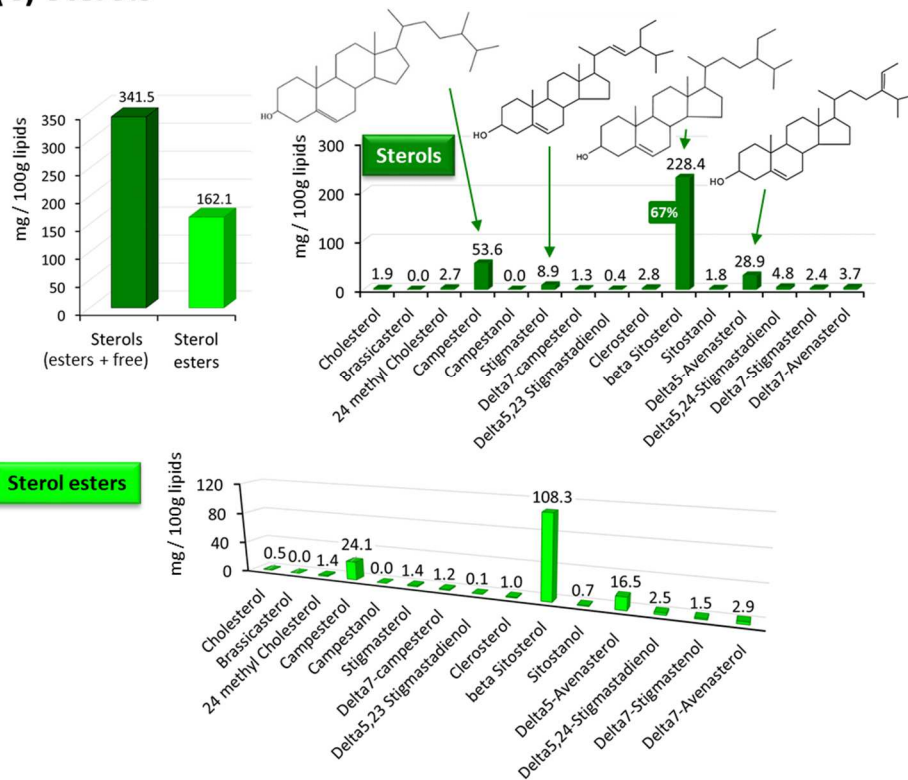
(A) Carotenoids



(B) Tocopherols and tocotrienols



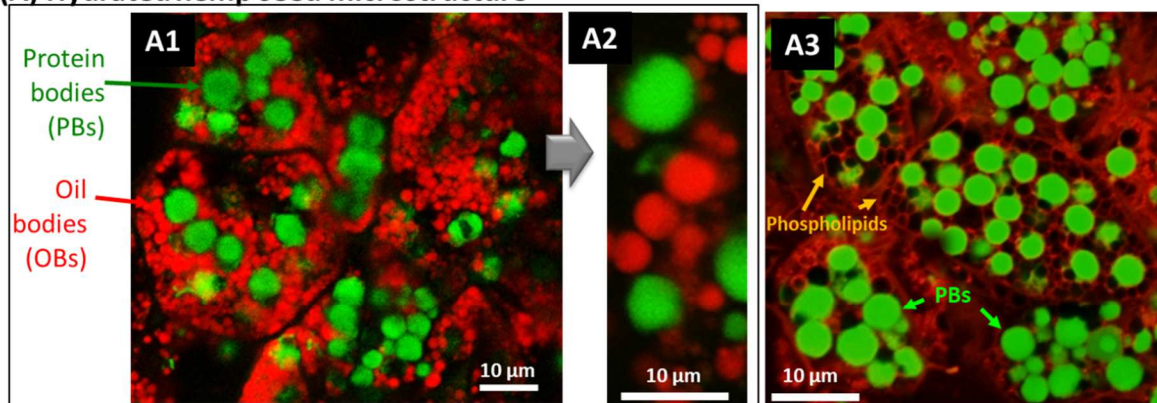
(C) Sterols



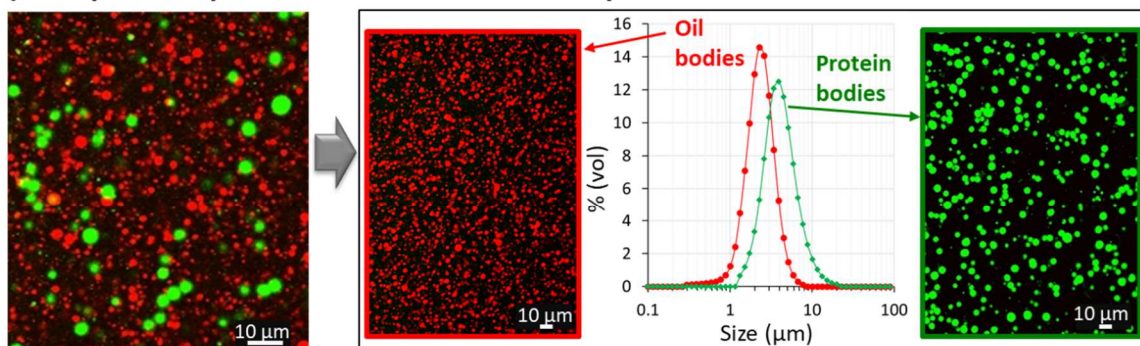
681

682 **Figure 3**

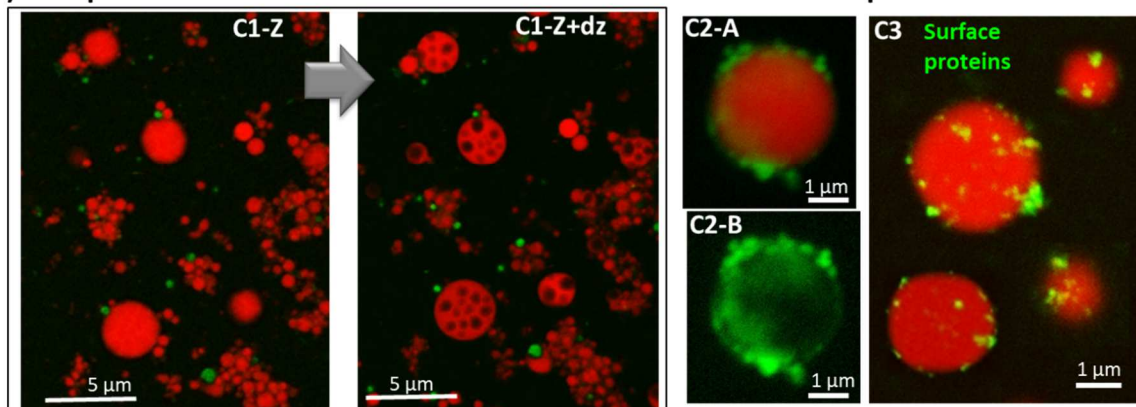
(A) Hydrated hemp seed microstructure



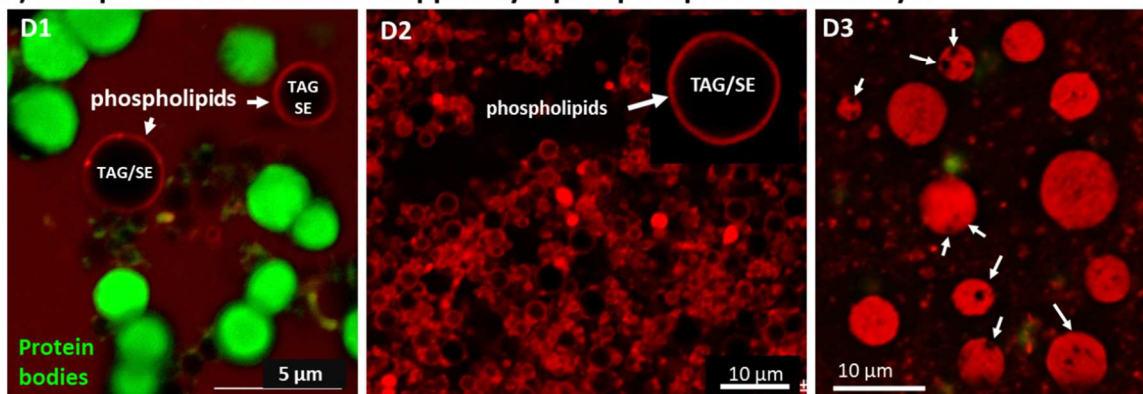
(B) Hemp seed aqueous extract: oil bodies and protein bodies



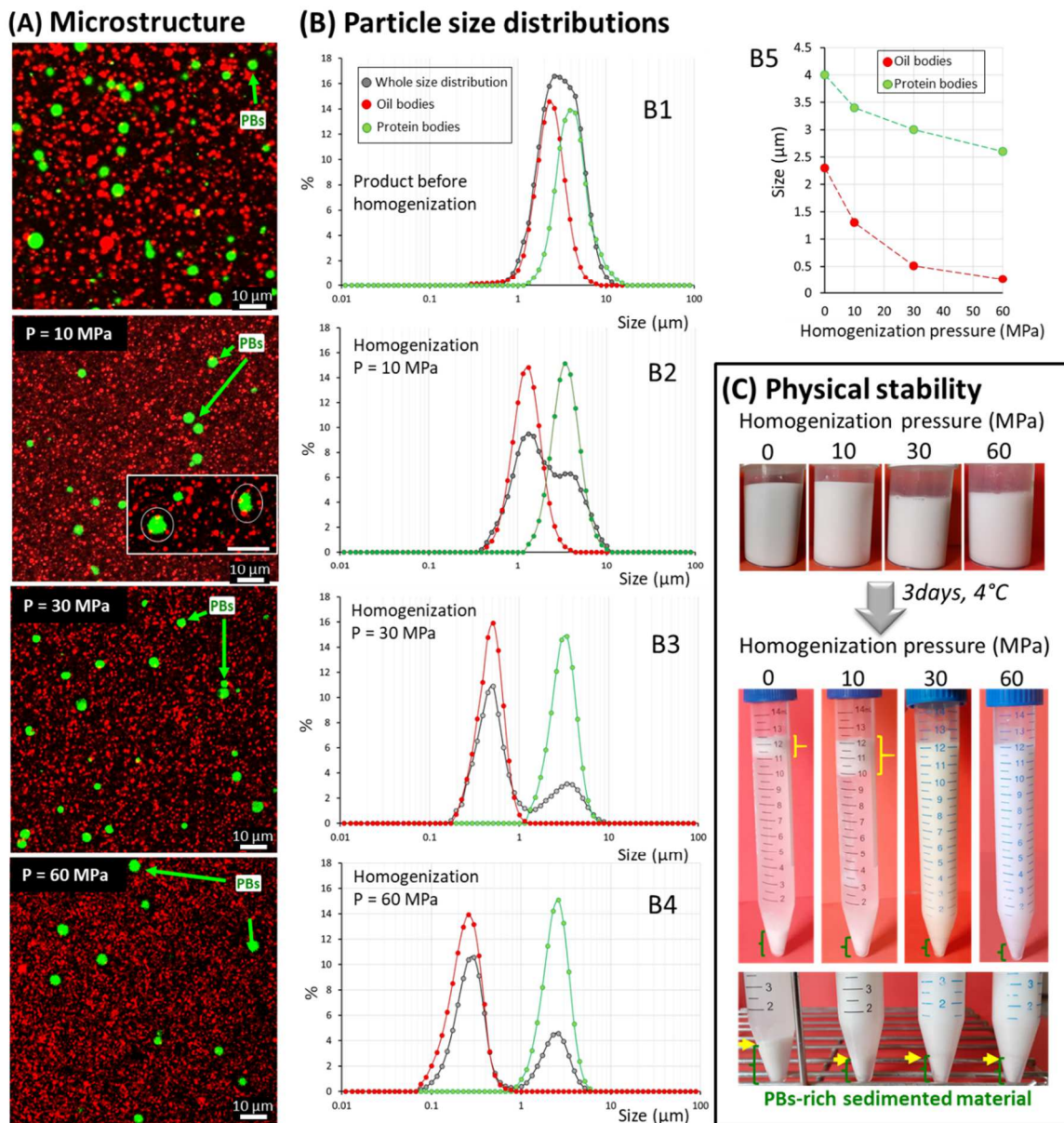
(C) Hemp seed oil bodies: TAG-rich core and membrane-associated proteins



(D) Hemp seed oil bodies envelopped by a phospholipid-rich monolayer



684 **Figure 4**



685

686

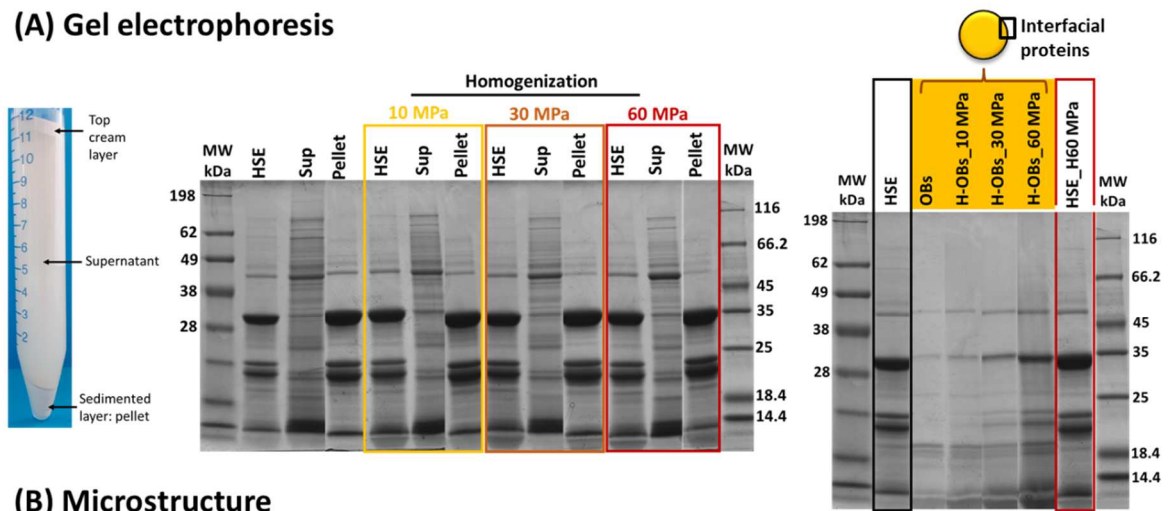
687

688

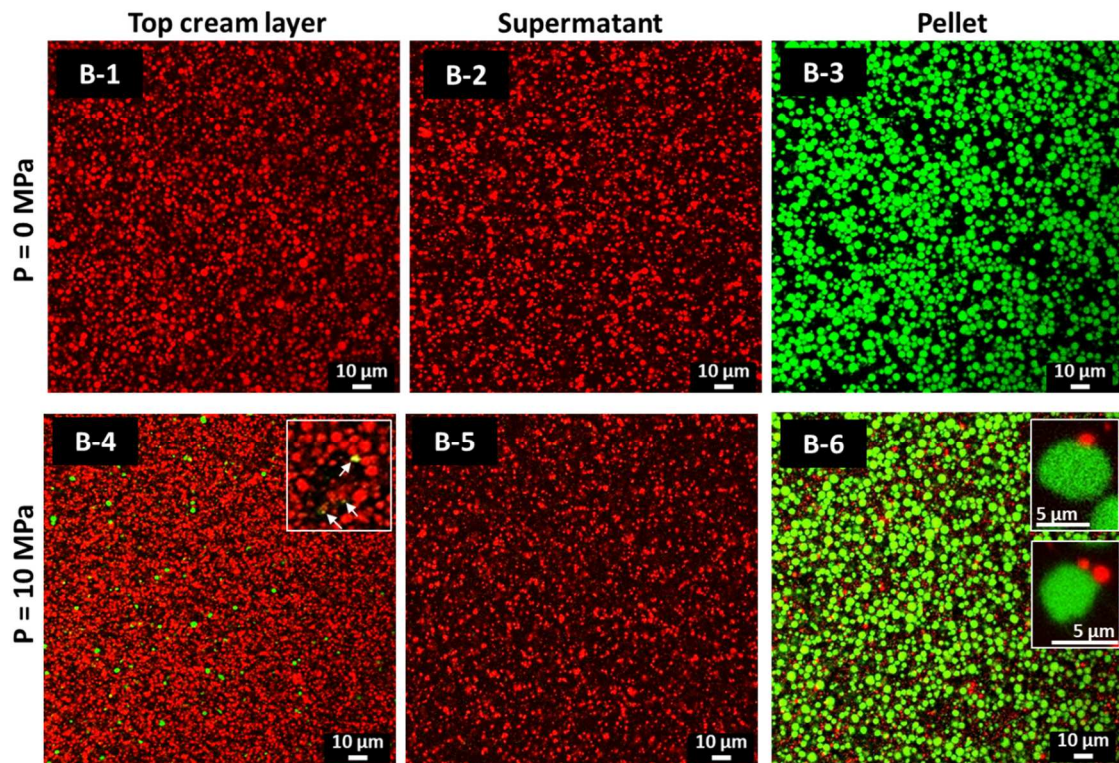
689 **Figure 5**

690

(A) Gel electrophoresis



(B) Microstructure



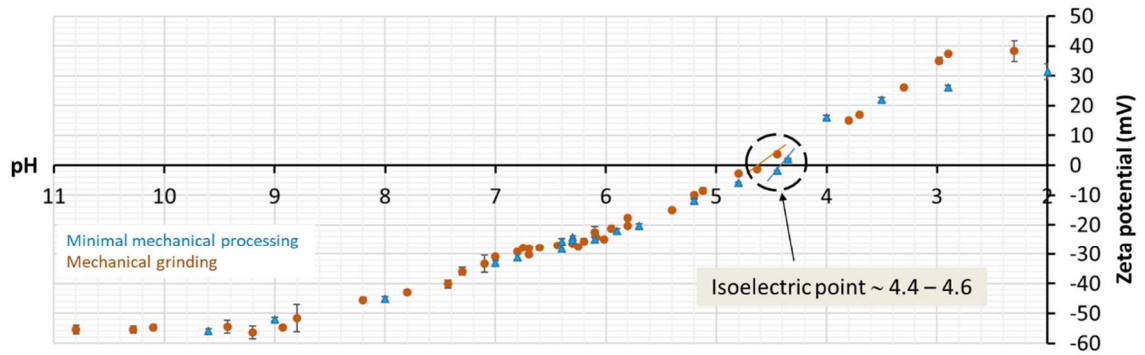
691

692

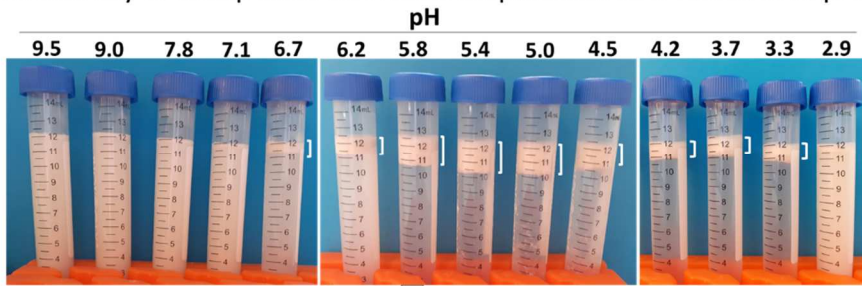
693

694 **Figure 6**

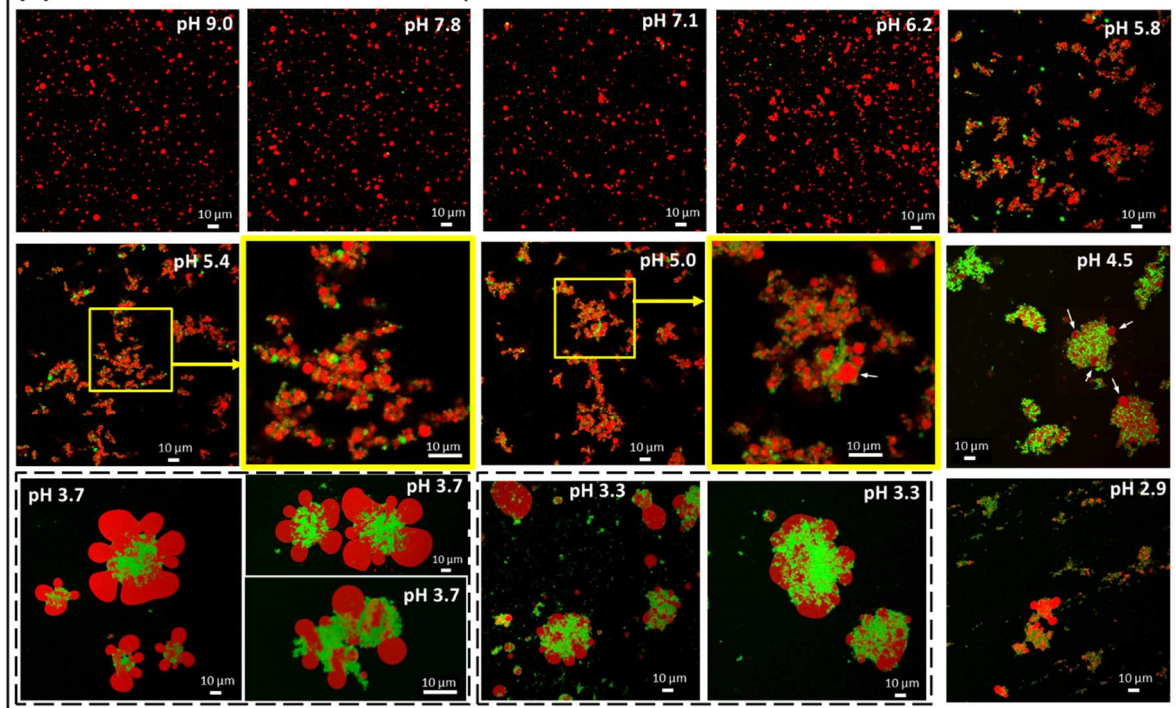
(A) Zeta potential as a function of pH



(B) Physical stability of hemp seed oil bodies suspensions as a function of pH



(C) Microstructure as a function of pH



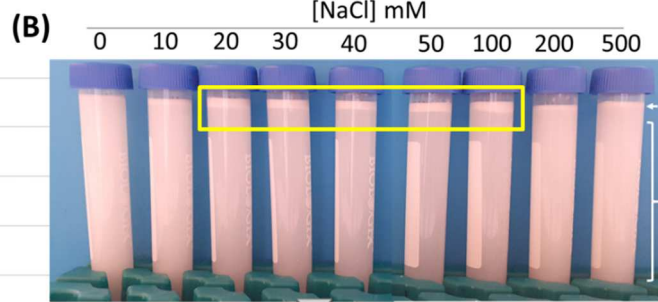
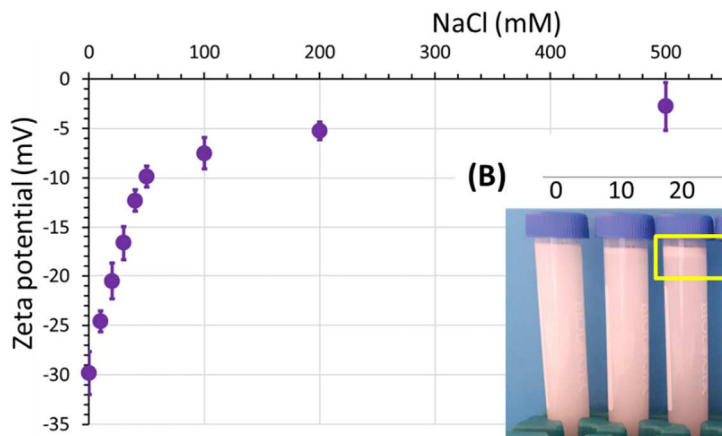
695

696

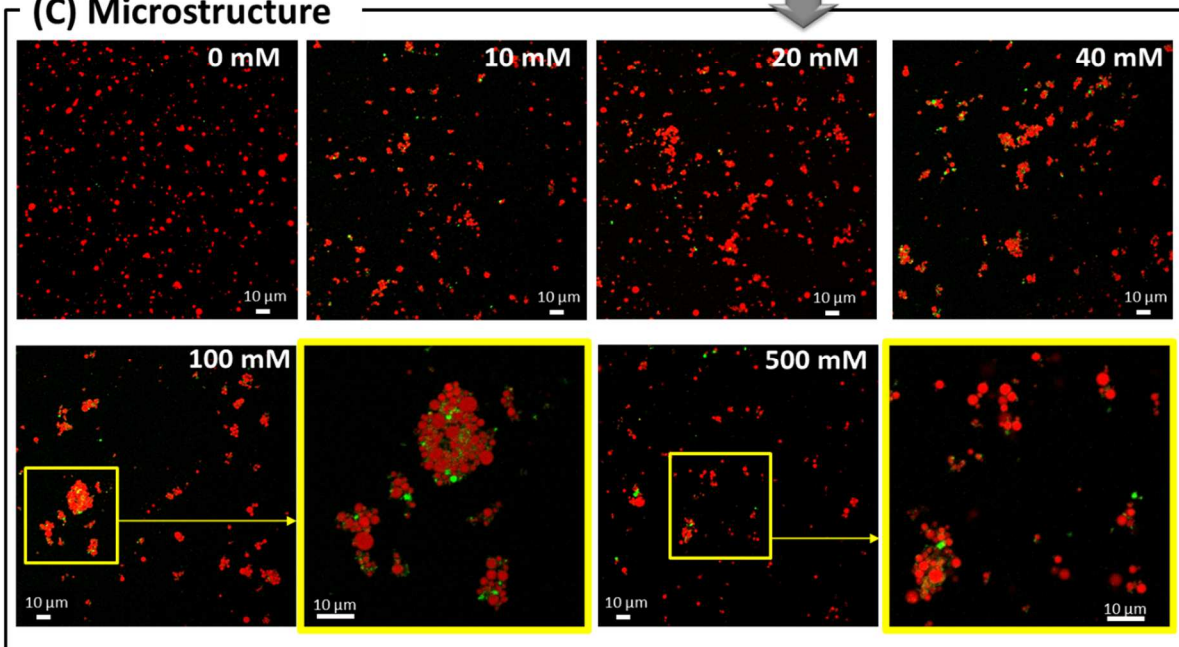
697

698 **Figure 7**

(A) Zeta potential as a function of NaCl concentration



(C) Microstructure



699

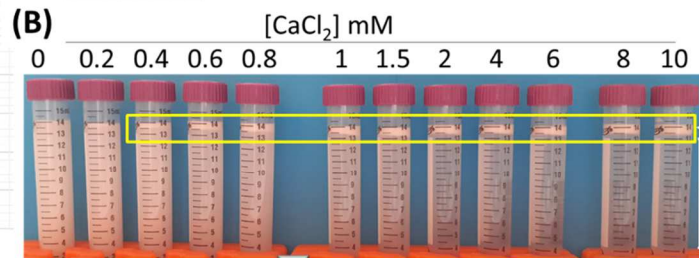
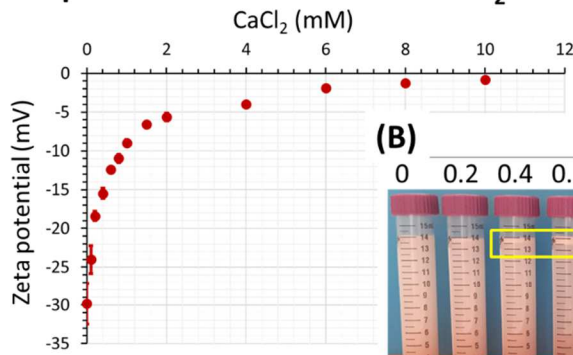
700

701

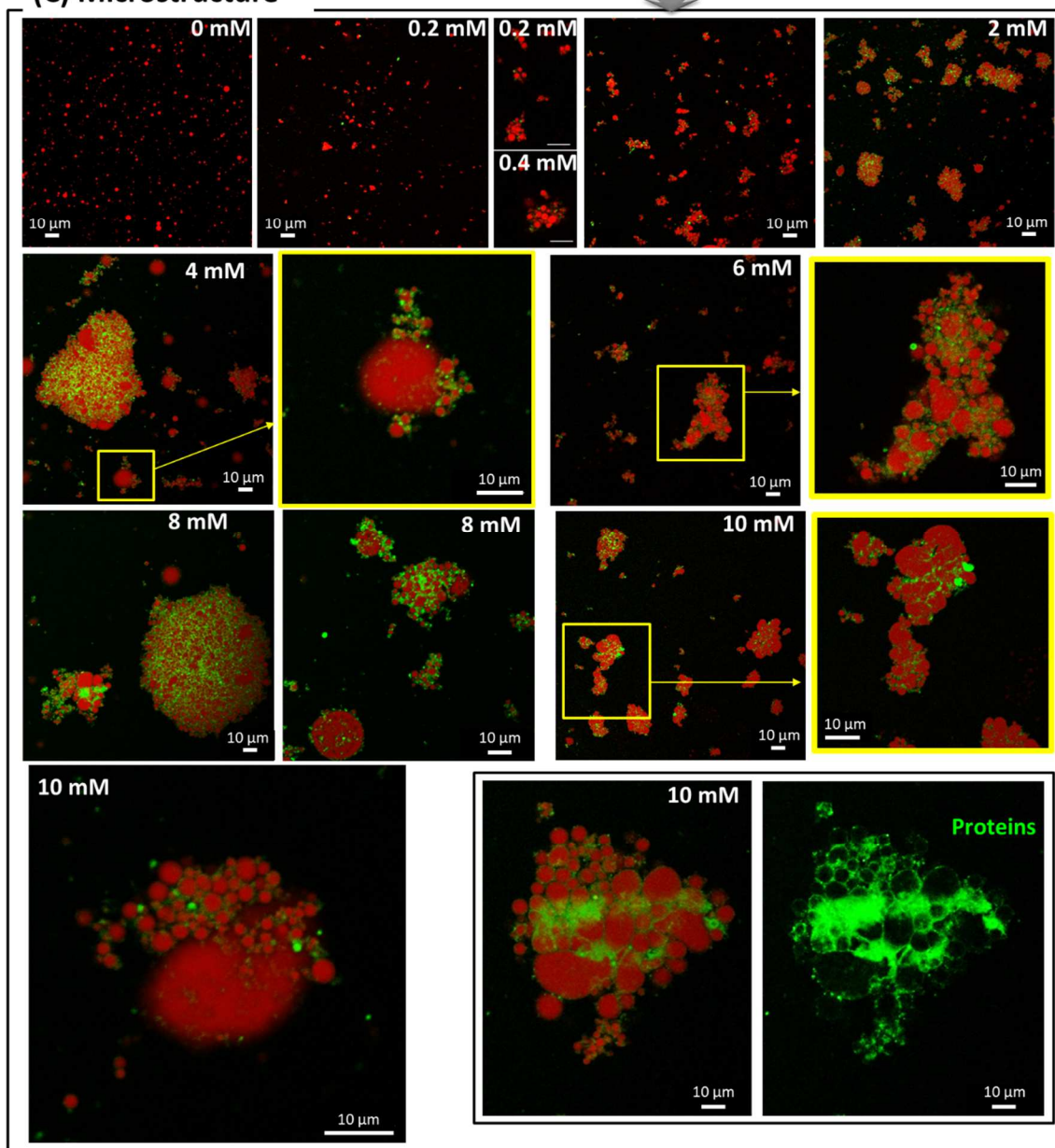
702

703 **Figure 8**

(A) Zeta potential as a function of CaCl₂ concentration



(C) Microstructure



704

705

706 **Reference list**

- 707 Acevedo-Fani, A., Dave, A., Singh, H., 2020. Nature-Assembled Structures for Delivery of Bioactive
708 Compounds and Their Potential in Functional Foods. *Front Chem* 8, 564021.
709 <https://doi.org/10.3389/fchem.2020.564021>
- 710 Antonelli, M., Benedetti, B., Cannazza, G., Cerrato, A., Citti, C., Montone, C.M., Piovesana, S., Laganà,
711 A., 2020. New insights in hemp chemical composition: a comprehensive polar lipidome
712 characterization by combining solid phase enrichment, high-resolution mass spectrometry,
713 and cheminformatics. *Anal Bioanal Chem* 412, 413–423. [https://doi.org/10.1007/s00216-
714 019-02247-6](https://doi.org/10.1007/s00216-019-02247-6)
- 715 Battacchi, D., Verkerk, R., Pellegrini, N., Fogliano, V., Steenbekkers, B., 2020. The state of the art of
716 food ingredients' naturalness evaluation: A review of proposed approaches and their relation
717 with consumer trends. *Trends in Food Science & Technology* 106, 434–444.
718 <https://doi.org/10.1016/j.tifs.2020.10.013>
- 719 Czabany, T., Wagner, A., Zweytick, D., Lohner, K., Leitner, E., Ingolic, E., Daum, G., 2008. Structural
720 and biochemical properties of lipid particles from the yeast *Saccharomyces cerevisiae*. *J Biol*
721 *Chem* 283, 17065–17074. <https://doi.org/10.1074/jbc.M800401200>
- 722 Dave, A.C., Ye, A., Singh, H., 2019. Structural and interfacial characteristics of oil bodies in coconuts
723 (*Cocos nucifera* L.). *Food Chemistry* 276, 129–139.
724 <https://doi.org/10.1016/j.foodchem.2018.09.125>
- 725 Farinon, B., Molinari, R., Costantini, L., Merendino, N., 2020. The Seed of Industrial Hemp (*Cannabis*
726 *sativa* L.): Nutritional Quality and Potential Functionality for Human Health and Nutrition.
727 *Nutrients* 12, 1935. <https://doi.org/10.3390/nu12071935>
- 728 Folch, J., Lees, M., Stanley, G.H.S., 1957. A Simple Method for the Isolation and Purification of Total
729 Lipides from Animal Tissues. *J. Biol. Chem.* 226, 497–509.
- 730 Furse, S., Liddell, S., Ortori, C.A., Williams, H., Neylon, D.C., Scott, D.J., Barrett, D.A., Gray, D.A., 2013.
731 The lipidome and proteome of oil bodies from *Helianthus annuus* (common sunflower). *J*
732 *Chem Biol* 6, 63–76. <https://doi.org/10.1007/s12154-012-0090-1>
- 733 Gallier, S., Gordon, K.C., Singh, H., 2012. Chemical and structural characterisation of almond oil
734 bodies and bovine milk fat globules. *Food Chemistry* 132, 1996–2006.
735 <https://doi.org/10.1016/j.foodchem.2011.12.038>
- 736 Huang, A.H.C., 1994. Structure of plant seed oil bodies. *Current Opinion in Structural Biology* 4, 493–
737 498. [https://doi.org/10.1016/S0959-440X\(94\)90210-0](https://doi.org/10.1016/S0959-440X(94)90210-0)
- 738 ISO 9936:2016, n.d. Corps gras d'origines animale et végétale — Détermination des teneurs en
739 tocophérols et en tocotriénols par chromatographie en phase liquide à haute performance
740 [WWW Document]. ISO. URL
741 [https://www.iso.org/cms/render/live/fr/sites/isoorg/contents/data/standard/06/95/69595.
742 html](https://www.iso.org/cms/render/live/fr/sites/isoorg/contents/data/standard/06/95/69595.html) (accessed 4.27.21).
- 743 ISO-8420, 2002. Animal and vegetable fats and oils — Determination of content of polar compounds
744 [WWW Document]. ISO. URL
745 [https://www.iso.org/cms/render/live/en/sites/isoorg/contents/data/standard/03/32/33289.
746 html](https://www.iso.org/cms/render/live/en/sites/isoorg/contents/data/standard/03/32/33289.html) (accessed 5.21.21).
- 747 ISO-122228-1, 2014. Determination of individual and total sterols contents — Gas chromatographic
748 method — Part 1: Animal and vegetable fats and oils [WWW Document]. ISO. URL
749 [https://www.iso.org/cms/render/live/en/sites/isoorg/contents/data/standard/06/02/60248.
750 html](https://www.iso.org/cms/render/live/en/sites/isoorg/contents/data/standard/06/02/60248.html) (accessed 5.21.21).
- 751 Israelachvili, J., 2011. *Intermolecular and Surface Forces - 3rd Edition*. Elsevier.
- 752 Kapchie, V.N., Yao, L., Hauck, C.C., Wang, T., Murphy, P.A., 2013. Oxidative stability of soybean oil in
753 oleosomes as affected by pH and iron. *Food Chem* 141, 2286–2293.
754 <https://doi.org/10.1016/j.foodchem.2013.05.018>

- 755 Laemmli, U.K., 1970. Cleavage of Structural Proteins during the Assembly of the Head of
756 Bacteriophage T4. *Nature* 227, 680–685. <https://doi.org/10.1038/227680a0>
- 757 Lawrence, A.-M., Besir, H., 2009. Staining of Proteins in Gels with Coomassie G-250 without Organic
758 Solvent and Acetic Acid. *J Vis Exp* 1350. <https://doi.org/10.3791/1350>
- 759 Lopez, C., Briard-Bion, V., Ménard, O., 2014. Polar lipids, sphingomyelin and long-chain unsaturated
760 fatty acids from the milk fat globule membrane are increased in milks produced by cows fed
761 fresh pasture based diet during spring. *Food Research International* 58, 59–68.
762 <https://doi.org/10.1016/j.foodres.2014.01.049>
- 763 Malomo, S.A., He, R., Aluko, R.E., 2014. Structural and functional properties of hemp seed protein
764 products. *J Food Sci* 79, C1512-1521. <https://doi.org/10.1111/1750-3841.12537>
- 765 Marsh, D., 2013. *Handbook of Lipid Bilayers*, 2nd édition. ed. CRC Press, Boca Raton, FL.
- 766 Maurer, S., Waschatko, G., Schach, D., Zielbauer, B.I., Dahl, J., Weidner, T., Bonn, M., Vilgis, T.A.,
767 2013. The role of intact oleosin for stabilization and function of oleosomes. *J Phys Chem B*
768 117, 13872–13883. <https://doi.org/10.1021/jp403893n>
- 769 Melcrová, A., Pokorna, S., Pullanchery, S., Kohagen, M., Jurkiewicz, P., Hof, M., Jungwirth, P., Cremer,
770 P.S., Cwiklik, L., 2016. The complex nature of calcium cation interactions with phospholipid
771 bilayers. *Scientific Reports* 6, 38035. <https://doi.org/10.1038/srep38035>
- 772 Montserrat-de la Paz, S., Marín-Aguilar, F., García-Giménez, M.D., Fernández-Arche, M.A., 2014.
773 Hemp (*Cannabis sativa* L.) seed oil: analytical and phytochemical characterization of the
774 unsaponifiable fraction. *J Agric Food Chem* 62, 1105–1110.
775 <https://doi.org/10.1021/jf404278q>
- 776 Naested, H., Frandsen, G.I., Jauh, G.Y., Hernandez-Pinzon, I., Nielsen, H.B., Murphy, D.J., Rogers, J.C.,
777 Mundy, J., 2000. Caleosins: Ca²⁺-binding proteins associated with lipid bodies. *Plant Mol Biol*
778 44, 463–476. <https://doi.org/10.1023/a:1026564411918>
- 779 NF-EN-12823-2, 2001. Foodstuffs - Determination of vitamin A by high performance liquid
780 chromatography - Part 2 : measurement of beta-carotene, NF EN 12823-2 - January 2001
781 [WWW Document]. URL [https://m.boutique.afnor.org/standard/nf-en-12823-2/foodstuffs-](https://m.boutique.afnor.org/standard/nf-en-12823-2/foodstuffs-determination-of-vitamin-a-by-high-performance-liquid-chromatography-part-2-measurement-of-beta-carotene/article/668832/fa045722)
782 [determination-of-vitamin-a-by-high-performance-liquid-chromatography-part-2-](https://m.boutique.afnor.org/standard/nf-en-12823-2/foodstuffs-determination-of-vitamin-a-by-high-performance-liquid-chromatography-part-2-measurement-of-beta-carotene/article/668832/fa045722)
783 [measurement-of-beta-carotene/article/668832/fa045722](https://m.boutique.afnor.org/standard/nf-en-12823-2/foodstuffs-determination-of-vitamin-a-by-high-performance-liquid-chromatography-part-2-measurement-of-beta-carotene/article/668832/fa045722) (accessed 5.27.21).
- 784 Nikiforidis, C.V., Kiosseoglou, V., 2009. Aqueous Extraction of Oil Bodies from Maize Germ (*Zea mays*)
785 and Characterization of the Resulting Natural Oil-in-Water Emulsion. *J. Agric. Food Chem.* 57,
786 5591–5596. <https://doi.org/10.1021/jf900771v>
- 787 Nikiforidis, C.V., Matsakidou, A., Kiosseoglou, V., 2014. Composition, properties and potential food
788 applications of natural emulsions and cream materials based on oil bodies. *RSC Advances* 4,
789 25067–25078. <https://doi.org/10.1039/C4RA00903G>
- 790 Ntone, E., Bitter, J.H., Nikiforidis, C.V., 2020. Not sequentially but simultaneously: Facile extraction of
791 proteins and oleosomes from oilseeds. *Food Hydrocolloids* 102, 105598.
792 <https://doi.org/10.1016/j.foodhyd.2019.105598>
- 793 Patton, S., Huston, G.E., 1986. A method for isolation of milk fat globules. *Lipids* 21, 170–174.
794 <https://doi.org/10.1007/BF02534441>
- 795 Potin, F., Saurel, R., 2020. Hemp Seed as a Source of Food Proteins, in: Crini, G., Lichtfouse, E. (Eds.),
796 *Sustainable Agriculture Reviews 42: Hemp Production and Applications*, Sustainable
797 *Agriculture Reviews*. Springer International Publishing, Cham, pp. 265–294.
798 https://doi.org/10.1007/978-3-030-41384-2_9
- 799 Purkrtova, Z., Le Bon, C., Kralova, B., Ropers, M.-H., Anton, M., Chardot, T., 2008. Caleosin of
800 *Arabidopsis thaliana*: Effect of Calcium on Functional and Structural Properties. *J. Agric. Food*
801 *Chem.* 56, 11217–11224. <https://doi.org/10.1021/jf802305b>
- 802 Qi, B., Ding, J., Wang, Z., Li, Y., Ma, C., Chen, F., Sui, X., Jiang, L., 2017. Deciphering the characteristics
803 of soybean oleosome-associated protein in maintaining the stability of oleosomes as affected
804 by pH. *Food Research International* 100, 551–557.
805 <https://doi.org/10.1016/j.foodres.2017.07.053>

- 806 Román, S., Sánchez-Siles, L.M., Siegrist, M., 2017. The importance of food naturalness for consumers:
807 Results of a systematic review. *Trends in Food Science & Technology* 67, 44–57.
808 <https://doi.org/10.1016/j.tifs.2017.06.010>
- 809 Romero-Guzmán, M.J., Köllmann, N., Zhang, L., Boom, R.M., Nikiforidis, C.V., 2020. Controlled
810 oleosome extraction to produce a plant-based mayonnaise-like emulsion using solely
811 rapeseed seeds. *LWT* 123, 109120. <https://doi.org/10.1016/j.lwt.2020.109120>
- 812 Rupasinghe, H.P.V., Davis, A., Kumar, S.K., Murray, B., Zheljzkov, V.D., 2020. Industrial Hemp
813 (*Cannabis sativa* subsp. *sativa*) as an Emerging Source for Value-Added Functional Food
814 Ingredients and Nutraceuticals. *Molecules* 25. <https://doi.org/10.3390/molecules25184078>
- 815 Sarkar, A., Dickinson, E., 2020. Sustainable food-grade Pickering emulsions stabilized by plant-based
816 particles. *Current Opinion in Colloid & Interface Science, Emulsions and Microemulsions* 49,
817 69–81. <https://doi.org/10.1016/j.cocis.2020.04.004>
- 818 Simopoulos, A.P., 2002. The importance of the ratio of omega-6/omega-3 essential fatty acids.
819 *Biomed Pharmacother* 56, 365–379. [https://doi.org/10.1016/s0753-3322\(02\)00253-6](https://doi.org/10.1016/s0753-3322(02)00253-6)
- 820 Smith, P.K., Krohn, R.I., Hermanson, G.T., Mallia, A.K., Gartner, F.H., Provenzano, M.D., Fujimoto, E.K.,
821 Goetze, N.M., Olson, B.J., Klenk, D.C., 1985. Measurement of protein using bicinchoninic acid.
822 *Analytical Biochemistry* 150, 76–85. [https://doi.org/10.1016/0003-2697\(85\)90442-7](https://doi.org/10.1016/0003-2697(85)90442-7)
- 823 Sorrentino, G., 2021. Introduction to emerging industrial applications of cannabis (*Cannabis sativa* L.).
824 *Rend Lincei Sci Fis Nat* 1–11. <https://doi.org/10.1007/s12210-021-00979-1>
- 825 St Angelo, A.J., Yatsu, L.Y., Altschul, A.M., 1968. Isolation of edestin from aleurone grains of *Cannabis*
826 *sativa*. *Arch Biochem Biophys* 124, 199–205. [https://doi.org/10.1016/0003-9861\(68\)90320-2](https://doi.org/10.1016/0003-9861(68)90320-2)
- 827 Tang, C.-H., Ten, Z., Wang, X.-S., Yang, X.-Q., 2006. Physicochemical and Functional Properties of
828 Hemp (*Cannabis sativa* L.) Protein Isolate. *J. Agric. Food Chem.* 54, 8945–8950.
829 <https://doi.org/10.1021/jf0619176>
- 830 Tully, R.E., Beevers, H., 1976. Protein Bodies of Castor Bean Endosperm: Isolation, Fractionation, and
831 the Characterization of Protein Components. *Plant Physiology* 58, 710–716.
832 <https://doi.org/10.1104/pp.58.6.710>
- 833 Tzen, J., Cao, Y., Laurent, P., Ratnayake, C., Huang, A., 1993. Lipids, Proteins, and Structure of Seed Oil
834 Bodies from Diverse Species. *Plant Physiol* 101, 267–276.
- 835 Tzen, J., Huang, A.H.C., 1992. Surface structure and properties of plant seed oil bodies. *J Cell Biol* 117,
836 327–335. <https://doi.org/10.1083/jcb.117.2.327>
- 837 Tzen, J.T., Lie, G.C., Huang, A.H., 1992. Characterization of the charged components and their
838 topology on the surface of plant seed oil bodies. *Journal of Biological Chemistry* 267, 15626–
839 15634. [https://doi.org/10.1016/S0021-9258\(19\)49582-3](https://doi.org/10.1016/S0021-9258(19)49582-3)
- 840 Wang, W., Cui, C., Wang, Q., Sun, C., Jiang, L., Hou, J., 2019. Effect of pH on physicochemical
841 properties of oil bodies from different oil crops. *J Food Sci Technol* 56, 49–58.
842 <https://doi.org/10.1007/s13197-018-3453-y>
- 843 White, D.A., Fisk, I.D., Mitchell, J.R., Wolf, B., Hill, S.E., Gray, D.A., 2008. Sunflower-seed oil body
844 emulsions: Rheology and stability assessment of a natural emulsion. *Food Hydrocolloids* 22,
845 1224–1232. <https://doi.org/10.1016/j.foodhyd.2007.07.004>
- 846 Wilschut, J., Duezguenes, N., Papahadjopoulos, D., 1981. Calcium/magnesium specificity in
847 membrane fusion: kinetics of aggregation and fusion of phosphatidylserine vesicles and the
848 role of bilayer curvature. *Biochemistry* 20, 3126–3133. <https://doi.org/10.1021/bj00514a022>
- 849 Yang, N., Su, C., Zhang, Y., Jia, J., Leheny, R.L., Nishinari, K., Fang, Y., Phillips, G.O., 2020. In situ
850 nanomechanical properties of natural oil bodies studied using atomic force microscopy.
851 *Journal of Colloid and Interface Science* 570, 362–374.
852 <https://doi.org/10.1016/j.jcis.2020.03.011>
- 853 Zaaboul, F., Raza, H., Chen, C., Liu, Y., 2018. Characterization of Peanut Oil Bodies Integral Proteins,
854 Lipids, and Their Associated Phytochemicals. *Journal of Food Science* 83, 93–100.
855 <https://doi.org/10.1111/1750-3841.13995>
- 856

857

858

Graphical abstract

